A Thermodynamic Analysis of the π^* and $E_T(30)$ Polarity Scales

Dmitry V. Matyushov,*,† Roland Schmid,‡ and Branka M. Ladanyi*,†

Department of Chemistry, Colorado State University, Fort Collins, Colorado 80523, and Institute of Inorganic Chemistry, Technical University of Vienna, Getreidemarkt 9, A-1060 Vienna, Austria

Received: June 4, 1996; In Final Form: October 1, 1996[⊗]

The solvent-induced UV−vis spectral shifts in 4-nitroanisole and pyridinium *N*-phenoxide betaine-30 dyes utilized in the famous π^* and $E_T(30)$ polarity scales, respectively, are analyzed by molecular theories in terms of long-range solute−solvent interactions due to induction, dispersion, and dipole−dipole forces. The solvent-induced shift is represented as a sum of the differential solute−solvent internal energy and the differential energy of binding the solvent molecules in the solute vicinity. The aim of the study is 3−fold: (i) to clarify and quantify the relative effects of the three types of interactions, (ii) to elicit the magnitude of the effect of specific forces, and (iii) to evaluate the contribution of the differential solvent binding to the spectral shift. For (i), the dye properties directing the weighting are the size and the differences in both polarizability and dipole moment between ground and excited states. Accordingly, the distinctions π^* vs $E_T(30)$ derive from the different sizes (4.5 vs 6.4 Å), dramatically different polarizability enhancement upon excitation (6 vs 61 Å^3), and opposite changes in the dipole moment (+8.2 vs −8.6 D) of the two dyes. As a key result, the importance of dispersion forces to the spectral shift even in highly polar liquids is emphasized. While the contributions of dispersions and inductions are comparable in the π^* scale, inductions are clearly overshadowed by dispersions in the $E_T(30)$ values. Both effects reinforce each other in π^*, producing the well-known red shift. For the $E_T(30)$ scale, the effects due to dispersion and dipolar solvation have opposite signs making the red shift for nonpolar solvents switch to the blue for polar solvents. For (ii), there is overall reasonable agreement between theory and experiment for both dyes, as far as the nonpolar and select solvents are concerned, but there are also discrepant solvent classes. Thus, the predicted $E_T(30)$ values for protic solvents are uniformly too low, revealing a decrease in H-bonding interactions of the excited state with lowered dipole moment. Further, the calculated π^* values of aromatic and chlorinated solvents are throughout too high, and this is explained by an increase in charge-transfer interactions of the more delocalized excited state. For (iii), the differential solvent binding energies have been extracted from experimental thermochromic data. For strongly polar fluids, the solute−solvent component of the shift overshadows that from the solvent binding energy variation. In nonpolar and weakly polar liquids the two parts are comparable for 4-nitroanisole, but the latter is still small for betaine-30. Experimental and calculated values in the present work parameters for betaine-30 are applied to calculating solvent reorganization energies λ_s of intramolecular electron transfer. λ_s is separated into polar activation by the solvent permanent dipoles and nonpolar activation due to induction and dispersion forces. Experimental reorganization energies due to the classical solvent and solute modes are throughout higher than the calculated λ_s values. The difference depends on solvent polarity and was attributed to the solute donor−acceptor vibrational mode coupled to the solvent polarization.

1. Introduction

The most popular word dealing with solvent effects is solvent polarity. Originally, this term was associated with solely the dielectric properties of the solvent but has assumed a broader meaning since the advent of the empirical solvent parameters[1−3] viewed to measure microscopic polarity (in contrast to the macroscopic dielectric constant). In this context, solvent polarity comprises all kinds of solvent−solute interactions.[3b] Although the success of empirical solvent parameters to account for medium effects on chemical reactivity[4] and many types of physicochemical properties is well-documented and appreciated, the underlying interpretations are often based more on intuition or preconceived opinion than on physically defined interaction mechanisms. As a matter of fact, the parameters used in multiparametric "linear solvation free energy relationships"[5] are not seldom interrelated,[4] featuring just different blends of fundamental intermolecular forces. In recent years another approach (which may be called the physical one in contrast to the chemical of above) to treating solvent effects is emerging, based on ideas derived from liquid state theories. This way of description is capable of significantly changing the traditionally accepted methods of research in chemistry and ultimately will lay the foundations of the understanding of chemical events from first principles. There is thus, for quite some time, great interest to making a connection between the empirical scales and theoretical, molecular-based models. In the present paper we set out to analyze two famous spectroscopic polarity scales, π^*[2,6] and $E_T(30)$,[3] based on the solvent-induced shift of electronic absorption transitions. The probe chromophores are 4-nitroanisole[7] for the former, and pyridinium *N*-phenoxide betaine-30 (betaine-30 below) for the latter. Apart from the great wealth of reliable experimental data, our choice was directed by more profound reasoning. First, the two chromophores are very different in size. In view of the divergent polarizabilities, they are expected to be differently sensitive to dispersion forces increasing with solute size. Second, the sign of the solvent polarity effect on the two scales is opposite. Betaine-30 is a negatively solvatochromic dye with the excited state dipole

† Colorado State University.
‡ Vienna Technical University.
[⊗] Abstract published in *Advance ACS Abstracts,* January 15, 1997.

S1089-5647(96)01609-4 CCC: $14.00

moment much lower than the ground state value which is the opposite to positively solvatochromic 4-nitroanisole. Since the dispersion forces would red shift the UV−vis spectral line, the dipolarity and dispersion effects counteract one another in E_T(30) but add up in π^*.

In the analysis we intend to calculate those components of the overall solvent effect that are amenable to adequate treatment, namely the components due to (i) induction, (ii) permanent dipoles' orientation, and (iii) dispersion. Induction forces are caused by the interaction of the permanent solute dipole with the solvent dipoles induced by the solute and solvent field. Dispersion forces are the result of the dipolar interactions between the virtually excited dipole moments of the solute and the solvent, resulting in a nonzero molecular polarizability. Both interaction mechanisms are therefore connected to the molecular electronic polarizability producing instantaneous (inertialess) equilibrium solvation in the course of optical excitation. However, the strength of the dispersion and induction solute−solvent coupling depends on the inertial solvent molecular coordinates. Their fluctuations (density fluctuations[8]) yield a reorganization (inertial) contribution to the solvent response, featured by the width of an optical spectral line or by the solvent reorganization energy in the electron transfer (ET) language. Apart from the solvent molecular coordinates, dipolar orientations comprising an inertial solvent mode remain equilibrated to the ground state solute charge distribution. It will thus be illuminating to see whether the description in terms of these "trivial" forces can afford the solvent dependence of the optical shifts. In this way other specific effects can be unraveled. Thus the following issues will be addressed: (1) What is the weighting of the individual intermolecular interactions in the overall solvent response? (2) What is the contribution of specific forces relative to nonspecific interactions? (3) What is the effect of the alteration of solvent−solvent interaction caused by optical excitation on spectral shift thermodynamics?

The first issue has been posed by recent studies of solvation in liquids, indicating that the traditional distinction between polar and nonpolar solvation is somewhat overemphasized. In contrast to the customary concepts of dipolar pathways, nonpolar solvation mechanisms, mainly based on dispersion forces, turn out to be an important contributor to solvation even in polar solvents. This has been established in equilibrium solvation calculations,[9] steady state,[6,10,11] and transient[12] spectroscopy as well as in closely related ET reactions in liquids.[13]

The second issue concerns the long-puzzling question in solution chemistry of the real impact of specific solute−solvent bindings on the solute spectral line. Of the two scales under scrutiny, the π^* values are viewed to measure the nonspecific part of the intermolecular interactions, while E_T(30) values involve also the solvent electrophilic solvation power, such as the hydrogen-bond ability and Lewis acidity.[3a] On the other hand, there are theories modeling the solvent shift in terms of only electrostatic interactions with the solvent taken as a continuum (and thus do not involve any specific interaction) and notwithstanding provide quite a good description when renormalized using the van der Waals (vdW) surface to give the solute radius.[14] Also, the simple Oshika−Bayliss−McRae analysis[15a,b] via continuum dielectric response functions reproduces quite well the spectral shifts through three adjustable parameters dependent on solvent classes.[6] This success is especially surprising in view of the known inability of continuum reaction field models to quantitatively assess the dipolarity[16] and dispersion[13a] components of solvation, tending to overestimate both. Thus the weighting of the individual contributions to the solvent shift drawn from such analyses is questionable. However, the very existence of such correlations would advocate the view that the main portion of the solvent response stems from trivial nonspecific dispersion and dipolar forces. Therefore, the analysis of spectral shifts in terms of long-range nonspecific interactions described by central intermolecular potentials may reveal whether such an approach can capture the essential physics of the solvent effect. In this way the portion due to specific solvent properties, like molecular anisotropy and participation in donor−acceptor interactions, may be extracted.

New insight into the third question has been brought about by recent studies on ionic[17] and nonpolar[18] solvation. A recent thermodynamic analysis[17b,19] shows that the free energy of solvation does not contain contributions from solvent−solvent correlations. On the other hand, the enthalpy and entropy of solvation are the sums of the solute−solvent, H_{0s} and S_{0s}, and the solvent reorganization, H_{ss} and S_{ss}, terms, the latter deriving from the perturbation of the solvent−solvent correlations by the solute. These reorganization contributions cancel each other exactly out in the free energy, i.e. $H_{ss} = TS_{ss}$.[17b,19] The new question arising with this picture concerns both the sign and the magnitude of the reorganization component H_{ss}. Analytical[17a] and simulation[17b] treatments of ion solvation yield positive values of H_{ss}, indicating a positive energetic strain produced by the solute. In the process of solvation the solute−solvent interactions are lowering the total system energy. This energy gain, however, is reduced, according to Le Chatelier's principle, by a concomitant increase in the average solvent−solvent interaction energy (softening of the solvent−solvent coupling) amounting to about half[17b] the solute−solvent stabilization energy. By contrast, the old "iceberg-formation" concept[18a] of nonpolar solvation predicts a strengthening of the solvent−solvent interactions, implying negative values of H_{ss} as has also been supported by molecular simulations.[18b−d] A recent study on methane hydration[18e] shows that the negative reorganization energy is located mainly in the first hydration shell. The dipolar solvation we consider here is intermediate in strength between ion and nonpolar solvation. Our previous analysis of dipole hydration thermodynamics yielded positive reorganization enthalpies.[28b] Unfortunately, the spectroscopic probe of the solvent response cannot in principle provide a support of this result, since it includes only *differential* reorganization energies (see section 2A below). However, the portion of the reorganization energy in the spectral shift gives the relative impact of solute−solvent vs solvent−solvent forces. We will extract the reorganization component from experimental data on absorption thermochromism.

The present analysis may also provide new perspectives on the closely related problem of thermally activated intramolecular ET reactions in liquids. Although the classical continuum formulations of both issues (optical transition and ET) emerged almost simultaneously[15,20] and have long been developing largely independently, there is now a growing desire to get a rigorous description in terms of intermolecular forces shifting the research of ET reactions toward model systems amenable to spectroscopic methods. It is the combination of steady state and transient optical spectroscopy that becomes a powerful method of studying elementary mechanisms of ET and testing theoretical concepts.[21−23] The classical treatments of ET and optical transition have been facing serious problems when extended to nonpolar and weakly polar solvents, since the classical reorganization energies observed are much higher than surmised from electrostatic interactions in linear dielectric formalisms. ET reorganization energies (not to be confused with the solvation reorganization energy mentioned above) due

to the classical nuclear modes, as extracted from band-shape analyses of absorption spectra in apolar liquids, were found to fall in the range 0.2−0.4 eV.[22−25] The further partitioning into internal vibrations and solvent degrees of freedom is however still uncertain. Following continuum treatments, the nonpolar part of solvent reorganization energy is usually taken to be zero.[21b,d] To the contrary, recent resonance Raman spectroscopy measurements, applied to quantify the intramolecular component, point to a rather high (0.2−0.3 V) contribution of the solvent component.[24,25] In view of the widespread interest in the ET problematics, we include in section 3C the calculations of solvent reorganization energies for betaine-30. This chromophore has been widely employed by Barbara and coworkers[21] in studying solvent effects on ET.

2. Calculation Procedure

A. General Relations. Instantaneous (on the nuclear time scale) optical excitation of the chromophore leads to a Franck−Condon state equilibrated to the inertialess electronic modes and inducing a state of strain for the inertial modes. The inertialess modes produce equilibrium solvation of the excited and ground states by induced solvent dipoles and specific coupling such as H-bonds and charge-transfer interactions. The strain of the inertial solvent modes provokes *differential* solvation caused by the interaction of the changes in the solute multipoles and polarizability with the frozen field of the solvent nuclear subsystem. This inertial strain has been subdivided by Bayliss and McRae[15b] into packing and orientational parts, with the former attributed to the variation of solute size upon excitation. Such a definition is, however, too restrictive, since the packing strain includes also the center-of-mass positions of the solvent molecules to be changed in going to the equilibrium configuration. This variation in the molecular coordinates has been shown to provide about one-third of the overall equilibrium[26] and dynamic[27] solvent responses, and we address this point in the calculations below.

Assuming the solvent electronic modes follow adiabatically the variation of the solute charge distribution, electronic optical transitions proceed between the states equilibrated to the instantaneous electronic solvent polarization. The corresponding free energies can be obtained by calculating the partial partition functions over the fast electronic solvent and solute degrees of freedom[28a] of the system Hamiltonian $H^{(i)}$

$$\exp[-\beta U^{(i)}] = Tr_{el}(\exp[-\beta H^{(i)}])$$

and generally have the form

$$U^{(i)} = I^{(i)} + U_{0s}{}^{(i)}(1, ..., N) + U_{ss}{}^{(i)}(1, ..., N)$$

where $i = 1$ refers to the ground and 2 to the excited state, respectively, 1, ..., N are the nuclear solvent coordinates including center-of-mass locations and molecular orientations, $I^{(i)}$ is the vacuum energy of the solute, and $\beta = 1/(k_B T)$. The solvent molecular coordinates are defined relative to the solute coordinate frame assumed to be fixed. This is a reasonable approximation for the heavy chromophores considered in the present paper.[36b] The solute−solvent $U_{0s}{}^{(i)}(1, ..., N)$ and solvent−solvent $U_{ss}{}^{(i)}(1, ..., N)$ interaction potentials are the functions of the coordinates of all N solvent molecules due to the nonpairwise coupling of the induced solvent and solute dipole moments. The classical and quantum components of the molecular polarizability tensor result, respectively, in induction and dispersion forces in $U_{0s}{}^{(i)}(1, ..., N)$ and $U_{ss}{}^{(i)}(1, ..., N)$.[28a] The latter are generally also nonpairwise.[29] The solute−solvent interaction potential may be pairwise decomposed in terms of the effective medium approach[30] replacing the polarizable liquid by a fictitious fluid of particles with effective permanent dipoles. This approach will be utilized below in section 2E when treating the dipolar component of the spectral shift. We also assume the pairwise form for the solute−solvent disperson forces in section 2D. The treatment of the solvent−solvent interaction energy $U_{ss}{}^{(i)}(1, ..., N)$ becomes, however, a more complicated problem when the solute polarizability is taken into account. In addition to the usual dipolar interaction, the solvent dipoles near the solute are coupled through the solute-induced dipole (this is explicitly shown in Appendix A for a model system of a dipolar polarizable solute in a dipolar polarizable solvent). This additional coupling of the solvent dipoles $\mathbf{m}_j$ and $\mathbf{m}_k$ is expressed by the three-particle solvent−solute−solvent term (eq A3 in Appendix A) $\alpha_0{}^{(i)}\mathbf{m}_j\cdot\mathbf{T}_{j0}\cdot\mathbf{T}_{0k}\cdot\mathbf{m}_k$ involving the product of two dipolar tensors $\mathbf{T}$ and thus effectively decaying as $\propto 1/r^6$ (actually as $\propto 1/(r_{0j}{}^3 r_{0k}{}^3)$) with the solute−solvent separation r (in our notations "0" always refers to the solute). Therefore, in order to express $U^{(i)}$ in terms of effective pairwise potentials, we have to introduce the inhomogeneous dependence of $U_{ss}{}^{(i)}(jk)$ on the solute−solvent distance and the solute state

$$U^{(i)} = I^{(i)} + \sum_j U_{0s}{}^{(i)}(j) + {}^1/_2 \sum_{j\neq k} U_{ss}{}^{(i)}(jk) \qquad (1)$$

The solute state dependence of the solvent−solvent interaction potential is thus a local property displaying itself only in the immediate vicinity of the solute. Being proportional to the solute polarizability, it may be significant only for highly polarizable chromophores.

The energies $U^{(i)}$ are the functions of the positions and orientations of the solvent molecules. In order to get the absorption frequency we need to average the instantaneous energy difference $\Delta U = U^{(2)} - U^{(1)}$ probed by optical excitation over the nuclear solvent configurations corresponding to the equilibrium ground state of the solute with the free energy $U^{(1)}$ (an analogous procedure is utilized in calculating the free energy surfaces of ET reactions[31]). The shift is thus split into the vacuum gap $\Delta = I^{(2)} - I^{(1)}$ and the differential solvation term. The latter is related to the variation of the solute−solvent $\sum_j \Delta U_{0s}(j)$ and solvent−solvent ${}^1/_2\sum_{j\neq k}\Delta U_{ss}$ interaction potentials and can be represented as follows

$$\hbar\omega_{abs} = \Delta + \rho\int \Delta U_{0s}(1) g_{0s}{}^{(1)}(1)\, d1 + \frac{\rho^2}{2}\int \Delta U_{ss}(12) g_{0ss}{}^{(1)}(12)\, d1\, d2 \qquad (2)$$

where $g_{0s}{}^{(1)}(1)$ and $g_{0ss}{}^{(1)}(12)$ are, respectively, the solute−solvent pair and solute−solvent−solvent triplet distribution functions in the initial ground state of the solute and ρ is the solvent number density. The second term in eq 2 can be rewritten by introducing the binding energy of the solvent molecules $B^{(i)}(1)$[18e]

$$g_{0s}{}^{(i)}(1)\, B^{(i)}(1) = \rho\int U_{ss}(12) g_{0ss}{}^{(i)}(12)\, d2$$

$B^{(i)}(1)$ determines average interaction energy of a solvent molecule at the distance r_1 from the solute and with the orientation ω_1 with the surrounding solvent molecules. In the $r_1 \rightarrow \infty$ limit $B^{(i)}(1)$ is independent of the molecular orientation and gives the bulk binding energy. The spectral shift is, however, affected by only the differential binding energy $\Delta B(1)$ quickly decaying with the distance from the solute

$$\hbar\omega_{abs} = \Delta + \Delta E_{0s} + \Delta E_{ss} \quad (3)$$

where

$$\Delta E_{0s} = \rho \int \Delta U_{0s}(1) g_{0s}(1)\, d1$$

and

$$\Delta E_{ss} = \frac{\rho}{2} \int g_{0s}^{(1)}(1) \Delta B^{(1)}(1)\, d1$$

The solvent-induced shift of the absorption energy involves thus the differential solute−solvent internal energy and the change in the solvent binding energy due to the instantaneous variation of the solvent−solvent potential near the solute. To the best of our knowledge, the latter component has not been previously included in spectral shift calculations. Because of the complexity of its theoretical assessment, we will extract ΔE_{ss} from experimental shifts by subtracting the calculated solute−solvent part ΔE_{0s} and from absorption thermochromism as shown below.

As follows from the thermodynamic perturbation analyses of Yu and Karplus,[17b] the shift is the internal energy component

$$\hbar\omega_{abs} = (\partial \beta \Delta F/\partial \beta)_V$$

of the differential Helmholtz free energy

$$\Delta F = \Delta + \int_0^1 d\lambda \int \Delta U_{0s}(1) g_{0s}^{(1)}(1;\lambda)\, d1 \quad (4)$$

where $g_{0s}^{(1)}(1;\lambda)$ for a general value of the coupling parameter λ refers to the ground solute state with the solute−solvent potential $\lambda U_{0s}^{(1)}$. As is seen in eq 4, the differential free energy ΔF arises as a result of the solute−solvent potential variation in the solute field charged from the zero value to the solute ground state value. ΔF is thus affected only by the solute−solvent interaction potential and does not contain the differential solvent binding term ΔE_{ss}. This term can therefore be extracted provided the difference $\hbar\omega_{abs} - \Delta F$ is known. This can be achieved by applying experimental temperature dependencies of absorption energies

$$\Delta F = (1/\beta) \int_0^\beta d\beta \hbar\omega_{abs}(\beta)$$

Experimental thermochromic data are commonly well-fitted by the linear form

$$\hbar\omega_{abs}(\beta) = a + b\beta$$

Then

$$\Delta F = a + (b/2)\beta$$

and

$$\hbar\omega_{abs} - \Delta F = (T/2)(\partial \hbar\omega_{abs}/\partial T)_V \quad (5)$$

Equation 5 provides a way of extracting the solvent binding term in the solvent-induced shift from experimental thermochromic data and the theoretically calculated ΔF and $\hbar\omega_{abs}$ values. However, spectral thermochromism is commonly measured at isobaric conditions. Therefore, we need to include the correction for the solvent expansibility resulting in

$$\hbar\omega_{abs} - \Delta F = T s_{abs}/2 - (\rho \alpha_p T/2)\left(\frac{\partial \hbar\omega_{abs}}{\partial \rho}\right)_T \quad (6)$$

where s_{abs} is the thermochromic absorption coefficient

$$s_{abs} = -\left(\frac{\partial \hbar\omega_{abs}}{\partial T}\right)_P$$

and α_p is the solvent isobaric expansibility.

The assessment of the solvent binding component of the spectral shift is also important for the related problem of intramolecular ET. The solvent ET reorganization energy defined as half of the Stokes shift is a sum of the solute−solvent $\lambda_s^{(0s)}$ and solvent−solvent $\lambda_s^{(ss)}$ parts

$$\lambda_s = \lambda_s^{(0s)} + \lambda_s^{(ss)} \quad (7)$$

where

$$\lambda_s^{(0s)} = \frac{\rho}{2} \int \Delta E_{0s}(1)[g_{0s}^{(1)}(1) - g_{0s}^{(2)}(1)]\, d1 \quad (8)$$

and

$$\lambda_s^{(ss)} = \frac{\rho}{4} \int [g_{0s}^{(1)}(1) \Delta B^{(1)}(1) - g_{0s}^{(2)}(1) \Delta B^{(2)}(1)]\, d1 \quad (9)$$

Whereas the first component is the standard ET reorganization energy due to the variation of the solute−solvent coupling, the second part is caused by the change in the solvent binding energy in the solute vicinity.

B. Model. The solvent influence on intramolecular optical excitation is treated here by implementing the perturbation expansion over the solute−solvent attractions. The reference system for the perturbation expansion is chosen to be the hard sphere (HS) liquid with the imbedded hard core of the solute. The main assumptions of our treatment are as follows:

(1) There is no electron overlap between solute and solvent; the solvent effect is only through long-range solute−solvent interactions.

(2) Excitation of the dye does not affect the exchange−repulsion solute−solvent interaction. This assumption will be reasonable for the bulky betaine-30 dye where electron density is buried inside the molecular core screening the solvent electrons but could break down for smaller chromophores[32] like 4-nitroanisole. In this case, the benzene π electron density may become capable of extending to the solvent region, and the repulsive solute−solvent coupling would affect the absorption energy.[32c] Actually, in their study of the solvent shift of vibronic transition in benzene, Stratt and Adams[33a,b] claimed that the inclusion of the repulsion size variation upon excitation is necessary for a correct description of the solvent shift in the range of densities from clusters to bulk solvent. A seemingly analogous result has recently been reported by Bader and Berne[33c] who simulated the optical transition of formaldehyde in water, suggesting an increase in the solute cavity radius by about 20% upon excitation. It should be noted, however, that the cavity radius defined by them as the first maximum of the solute−solvent distribution function incorporates not only the effect of repulsion forces involved in the traditional determinations of the cavity size but results from a balance between repulsions and multipole attractions.[34] The radius variation with excitation reflects thus in an effective manner the change in the local solvent density around the solute, considered previously in terms of a perturbation expansion.[26]

(3) We will utilize central two-particle interaction potentials for both solvent−solvent and solute−solvent interactions. This assumption concerns primarily the calculation of the solute−solvent dispersion energy. However, with accurate solvent Lennard−Jones (LJ) energies now available,[28a] the procedure has been shown to reproduce pretty well the experimental free

energies of dipolar solvation in a range of nonpolar and polar solvents.[28b] Also, the central potential approach compares favorably with the presumably more accurate algorithm based on adding up the dispersive contributions from individual solvating groups of the solvent.[11b]

(4) We include only molecular dipole moments of both solute and solvent and disregard higher multipoles. Further, solute and solvent are taken to have isotropic molecular polarizabilities.

(5) No specific solute−solvent and solvent−solvent interactions are considered.

As already mentioned, the purpose of applying this rather simplified model is 3−fold: (i) to determine how well the description in terms of trivial dipolar and dispersion forces can reproduce the solvent dependence of optical spectral shifts, (ii) to examine the solvent polarity dependence of dispersion and dipolar contributions to the energy shifts, and (iii) to extract the relative importance of more specific molecular properties. Our approach captures some physically important features of the effect of solvent on the electronic transitions in optical dyes hitherto neglected, fully or partially, in simulation techniques purported to provide a more detailed picture. Thus we include (i) nonzero polarizabilities of the solvent and solute and (ii) state dependence of the solute polarizability, permitting us to treat the dispersion contribution to the solvent−induced shift. In fact, the effect of solute and solvent polarizabilities has become increasingly appreciated in equilibrium[33c,35] and dynamic[36] computation techniques.

The solvation term in eq 2 for the absorption energy can be represented as a sum of the variation in the solute−solvent repulsion internal energy ΔE_{rep} and the contribution from the attraction forces. This latter component, due to different symmetries of the intermolecular potentials, can be split into the radial and angle dependent parts. The former is attributed to dispersions, ΔE_{disp}, and the latter to dipolar interactions, ΔE_p. Thus we get for the absorption energy

$$\hbar\omega_{abs} = \Delta + \Delta E_{rep} + \Delta E_{disp} + \Delta E_p + \Delta E_{ss} \qquad (10)$$

According to assumption (2) above, $\Delta E_{rep} = 0$. In the first nonvanishing term of the perturbation treatment, the dispersion and dipolarity components of the differential free energy ΔF and the internal energy ΔE_{0s} are connected by the simple relations

$$\Delta F_{disp} = \Delta E_{disp} \qquad \Delta F_p = {}^1/_2 \Delta E_p$$

We can thus rewrite eq 5 as follows

$$\Delta E_{ss} = (Ts_{abs} - \Delta E_p)/2 + (\rho\alpha_p T/2)\left(\frac{\partial \hbar\omega_{abs}}{\partial \rho}\right)_T \qquad (11)$$

which makes the calculation of the reorganization component of the solvent shift straightforward without involvement of dispersion solvation. Note, however, that whereas eq 5 is rather general, eq 11 is restricted to a perturbation treatment of dispersion and dipolar solvation to a lowest nonvanishing order. Equation 11 has an important advantage that it does not include the dispersion component of the shift. Therefore, it is not affected by the value of the solute polarizability change (without exclusion for the relatively small expansibility term which will be omitted in the calculations below) evaluated below by fitting absorption energies in nonpolar (4-nitroanisole) and weakly polar (betaine-30) solvents.

The perturbation expansion when applied to eqs 7−9 results in the always positive solute−solvent term $\lambda_s^{(0s)} \propto \Delta U_{0s}^2$ and the solvent binding term which sign is governed by the product $\Delta U_{ss}\Delta U_{0s}$. Since ΔU_{ss} is proportional to the solute polarizability variation (see Appendix A), the sign of $\lambda_s^{(ss)}$ is determined by $\Delta\alpha\Delta m$, where Δm is the solute dipole moment variation. Since molecular polarizability generally increases with optical excitations, $\lambda_s^{(ss)}$ should be positive for positively solvatochromic dyes and negative for negatively solvatochromic dyes.

C. Solute Effective Radius. The chromophores are generally nonspherical objects. The calculation of the solute−solvent response for such solutes is a difficult problem solved commonly by complicated computational algorithms,[37] empirical models,[38] or in terms of the interaction−site formalism.[40,41] Here we follow the more traditional approach replacing the nonspherical solute with an effective sphere of the radius to be determined through well−developed methods of liquid state theory. The guiding principle in our method of determining the effective radius is the observation that the main portion of the solvent effect in equilibrium solvation[9a] and spectral shift[39] stems from the first solvation shell. Local packing of the solvent around the chromophore, thus of utmost significance, has to be accommodated in average by the effectively spherical solute. The local packing due to the repulsive cores of the solvent molecules about the solute is reflected by the cavity formation energy defined as the free energy invested to create a cavity for the solute. We therefore suggest to evaluate the effective solute radius R_0 from the condition of equality between the cavity formation energy of the nonspherical, ΔG_{nsph}, and effectively spherical, $\Delta G_{sph}(d, \eta)$, solutes

$$\Delta G_{nsph} = \Delta G_{sph}(d, \eta) \qquad (12)$$

The free energy $\Delta G_{sph}(d, \eta)$ of spherical cavity formation in a HS liquid of diameter σ is taken here in the Boublik−Mansoori−Carnahan−Starling−Leland (BMCSL) form,[42] agreeing excellently with HS simulations.[43] The energy $\Delta G_{sph}(d, \eta)$ is a function of the solute−solvent size ratio, $d = 2R_0/\sigma$, and the liquid packing density $\eta = (\pi/6)\rho\sigma^3$. This definition of the effective solute radius is somewhat analogous to that proposed by Ravi et al.[44] who applied the volume excluded by the solute from the solvent to define the effective radius. Their approach is in fact a low-density limit of ours.

Before applying eq 12, the nonspherical solute geometry has to be defined, for which the cavity formation energy is evaluated. The elongated 4-nitroanisole chromophore is modeled here by a spherocylinder formed by two spheres of radius R_s with the centers separated by the distance R. The vdW radius of the benzene moiety in 4-nitroanisole equal to 2.633 Å is assigned to R_s. The separation R is equated to the distance between the oxygen and nitrogen sites of 4-nitroanisole estimated as 5.6 Å. On the basis of these assignments, we calculated the cavity formation energy $\Delta G_{nsph}(R_s, R, \sigma, \rho)$ of this spherocylinder from scaled particle theory.[45] By equating $\Delta G_{nsph}(R_s, R, \sigma, \rho)$ to the BMCSL energy we get, depending on the solvent considered, R_0 in the range 4.4−4.6 Å. This is very close to the independent quantum-mechanical estimate $R_0 = 4.6$ Å[46] for 4-nitroanisole and $R_0 = 4.4$ Å for the similar 4-azoxyanisole molecule.[47] Notice that the solute radius calculated from the mass density of the solute is much lower, $R_0 = 3.68$ Å. This estimate, although sometimes used,[48] is inadequate because of the more effective packing of elongated solute molecules in the condensed phase than that which could be expected from a simple spherical representation.

Following recent calculations of the spectral shift of the betaine chromophore in the framework of the extended reference interaction site method,[41] we model the betaine molecule by a pair of fused hard spheres with the radii $R_1 = 5$ Å and $R_s = 5.68$ Å separated by the distance $R = 4.223$ Å. The cavity

formation energy of a pair of fused HSs is taken according to Ben-Amotz and Herschbach.[49] The application of eq 12 then yields a value for R_0 that varies slightly with solvent in the range 6.3−6.5 Å, somewhat above the continuum-based spectroscopic estimate $R_0 = 6.2$ Å.[50]

D. The Dispersion Contribution. The intermolecular dispersive solute−solvent attractions are determined here on the basis of the London form of the C_6 dispersion coefficients. This approach based on two-particle central potentials has the advantage of incorporating the state dependence of dispersion forces. Several modifications of the original two-particle London potential are currently employed in the application to condensed phase calculations. One method, used also in computation techniques,[51] is based on ideas of Linder[52] and determines the solute−solvent dispersions through the Onsager reaction field. Another approach[53] makes use of the old Longuet-Higgins/Pople theory[53a] for treating vdW clusters[53b,c,d] and spectral shifts in polymer glasses.[11b] In that model, the solute polarizability, following Longuet-Higgins/Pople, is supposed to be unaffected by excitation and the variation of the excited, C_6^e, relative to the ground, C_6^g, dispersion coefficient is related to the change in the spectrum of solute virtual excitations. The ratio of the two coefficients is thus

$$C_6^{\,e}/C_6^{\,g} = 1 + \Delta/(I_0 + I_s)$$

where I_0 and I_s are the average excitation energies of solute and solvent, respectively, and Δ is the solute transition energy. However, as pointed out by Kakitani,[54] the variation of the virtual excitation spectrum is already included in the solute polarizability[55] and the difference of the dispersion coefficients is more correctly given in the form

$$C_6^{\,e} - C_6^{\,g} = {}^3/_2 I_s \alpha_s \left[\frac{I_0^{\,e}\alpha_e}{I_0^{\,e} + I_s} - \frac{I_0^{\,g}\alpha_g}{I_0^{\,g} + I_s}\right]$$

where I_0^e, α_e and I_0^g, α_g refer to the excited and ground states, respectively. If the optical transition considered is separated from other solute excitations, it is prudent to put $I_0^g = I_0^e = \Delta$. In this case,

$$C_6^{\,e} - C_6^{\,g} = {}^3/_2 \frac{I_s \Delta}{\Delta + I_s} \alpha_s \Delta\alpha \qquad (13)$$

This assumption is very restrictive and the difference in the solute polarizabilities $\Delta\alpha = \alpha_e - \alpha_g$ should generally be viewed as an effective parameter including the variation in both the polarization and the average excitation energy of the solute. Further, the assumption of Longuet-Higgins/Pople of the constancy of the solute polarizability in optical transitions is not supported by quantum-mechanical calculations.[56] For large and particularly for conjugated[56e] chromophores, optical transition may result in excited state polarizabilities that are several times higher than the ground state values. The polarizability of even an atom may change considerably with excitation,[57] e.g. for helium the scalar atomic polarizability changes from 0.205 Å^3 in the ground state to −8.86 Å^3 in the 2^1P and 7.34 Å^3 in 2^3P excited states, respectively.[57a] Similarly, the polarizability of lithium varies from 24 Å^3 in the 2^2S ground state to 6.8 Å^3 in the 2^4P^0 excited state.[57b] It seems therefore more appropriate to treat the alteration of the solute−solvent dispersion forces in terms of variable solute polarizability.

The shift of the transition band due to dispersion forces, ΔE_{disp}, is determined here from eq 13 in the perturbation expansion over the variation of the solute−solvent dispersion potential taken in the LJ form

$$\Delta u_{LJ}^{(0s)} = \frac{2\Delta}{\Delta + I_s}\left(\frac{\Delta\alpha}{\alpha_s}\right) u^{(0s)}(r), \quad u^{(0s)}(r) = 4\epsilon_{LJ}^{(s)}\left(\frac{\sigma_{LJ}^{(s)}}{\sigma_{LJ}^{(0s)}}\right)^6 [(\sigma_{LJ}^{(0s)}/r)^{12} - (\sigma_{LJ}^{(0s)}/r)^6]$$

where $\epsilon_{LJ}^{(s)}$ and α_s are the solvent LJ energy and polarizability, respectively. The solute−solvent diameter $\sigma_{LJ}^{(0s)} = R_0 + \sigma_{LJ}^{(s)}/2$ is defined as the combination of the solute radius and the liquid LJ diameter $\sigma_{LJ}^{(s)}$. The dispersions-induced shift is thus given by the relation[13a]

$$\Delta E_{disp} = \Delta\alpha\delta, \quad \delta = \frac{2\Delta}{\Delta + I_s}\left(\frac{\rho}{\alpha_s}\right)\int u^{(0s)}(r) g_{0s}^{(0)}(r)\, d\mathbf{r} \qquad (14)$$

where, according to our choice of the HS reference system, $g_{0s}^{(0)}(r)$ is the HS solute−solvent pair distribution function.

The variation of the solute polarizability (or, more exactly, the effective strength of solute−solvent dispersion forces) is difficult to estimate. We will gain the parameter $\Delta\alpha$ as the slope of the solvent variation of the energy

$$\Delta + \Delta E_{disp} = \hbar\omega_{abs} - \Delta E_p - \Delta E_{ss} \qquad (15)$$

obtained from experimental absorption energies in a range of solvents vs the calculated parameter δ. To guard ourselves against possible errors in calculating the dipolar part ΔE_p in eq 15, we will utilize only nonpolar (for π^*) or weakly polar [for $E_T(30)$] solvents with I_s energies equated with solvent ionization potentials,[58] as is traditional. Slope and intercept of such a plot provide us with the parameter $\Delta\alpha$ and the vacuum energy gap Δ, respectively. Since δ in eq 14 is by itself dependent on Δ, several iterations are necessary. The procedure is somewhat analogous to the calculation of solvent LJ energies from solubilities of inert gases in the Pierotti theory.[59] Yet, instead of using the continuum approximation of Pierotti model, it involves a molecular determination of δ as already successfully applied to extracting the $\Delta\alpha$ parameter in ET applications.[13b]

Figure 1a shows the plot of $\hbar\omega_{abs} - \Delta E_p$ and $\hbar\omega_{abs} - \Delta E_p - \Delta E_{ss}$ vs δ from eq 14 drawn for 4-nitroanisole in alkane solvents, using experimental values from refs 2c and 3b. The gas phase properties of the solvents have been listed in our previous paper[60] as well as the liquid state properties, HS diameters,[60] and LJ energies[28a] needed for the calculations. The differential energies of solvent binding ΔE_{ss} are evaluated from eq 11 using experimental thermochromic data[2b] and listed in Table 3. Involvement of ΔE_{ss} affects noticeably the calculation of $\Delta\alpha$ and Δ: we get $\Delta\alpha = 3.38$ Å^3 and $\Delta = 4.38$ eV without including ΔE_{ss} and $\Delta\alpha = 6.04$ Å^3 and $\Delta = 4.49$ eV with ΔE_{ss}. The latter value of Δ is closer to the experimental vacuum absorption energy 4.57 eV[2d] and the results of that analysis will be accepted for the subsequent calculations. Notice that the solute polarizability variation is small compared to the reported ground state value, $\alpha_0 = 15$ Å^3.[61] The effect of dispersion forces on the π^* absorption shift can therefore be only moderate (see below).

For the $E_T(30)$ polarity scale, due to solubility limits, direct experimental measurements in nonpolar liquids are not available. The tabulated values were derived from data of the more lipophilic $E_T(37)$ dye,[3b] showing no variation in the *n*-alkane series. This invariance, however, is highly suspicious, since the LJ energies increase strongly in moving up the *n*-alkane series.[28a] This has to mean that either the dispersion contribu-

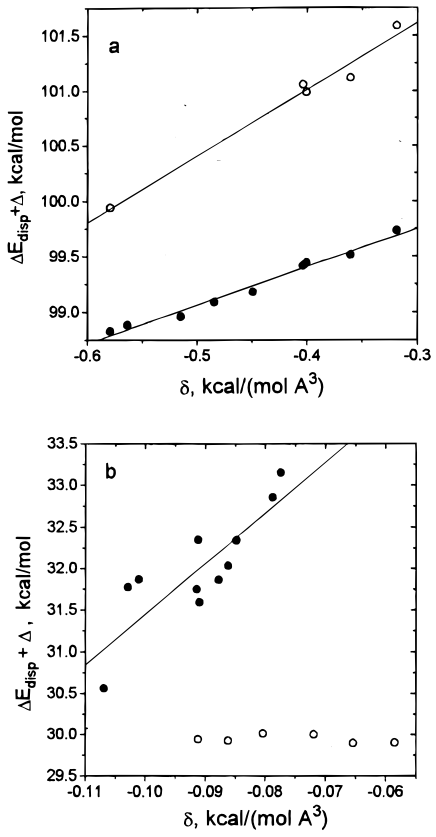

Figure 1. Plots of the dispersion and vacuum parts $\Delta + \Delta E_{disp}$ of the experimental UV−vis absorption shifts of 4-nitroanisole in alkanes (a) and of betaine-30 in weakly polar liquids (b) vs the parameter δ of solute−solvent dispersion attractions, eq 14. In (a), solid circles (●) correspond to the analysis without and open circles (○) with the differential binding energy ΔE_{ss}. Open circles (○) in (b) show the *n*-alkanes *n*-C_5−C_{10} with absorption energies derived from the correlation analysis.[3b] The solid lines show the best-fit linear regressions.

TABLE 1: Solute Parameters

solute	R_0,[a] Å	α_0, Å^3	$\Delta\alpha$, Å^3	m_g, D	m_e, D	Δ, eV
betaine-30	6.3−6.5	68	61	14.8	6.2	1.624
4-nitroanisole	4.4−4.6	15	6	4.7	12.9	4.49

[a] From eq 12, slightly solvent dependent.

tions to $E_T(30)$ are very small or the $E_T(30)$ values for nonpolar liquids are erroneous. In order to get rid of additional assumptions and to provide a more experimentally based test of the nonpolar $E_T(30)$ data, we utilized in the $\Delta\alpha$-analysis the 11 least polar liquids for which experimental $E_T(30)$ data are available. Because of the scarcity of experimental thermochromic data for betaine-30 in nonpolar fluids, we cannot include ΔE_{ss} values in the $\Delta\alpha$-analysis. They are, however, expected to be smaller than those for 4-nitroanisole as can be judged from examining the existing data for the nonpolar aromatic solvents given in Table 3. The plot of $\hbar\omega_{abs} - \Delta E_p$ vs δ in Figure 1b, though noticeably scattered, yields $\Delta\alpha = 61$ Å^3. The intercept amounts to $\Delta = 1.624$ eV, substantially higher than the reported value of 1.175 eV.[3b] Notice, however, that this latter figure was not obtained from direct experimental measurement, but instead from a secondary analysis of the correlation between an isomerization reaction and $E_T(30)$ values.[3d] Apparent support of such a low value was purported to be provided by a solvent spectral shift analysis,[62] which, however, considered only the dipolar part of the spectral shift (and disregarded the dispersion forces contributions). Although the MSA-based analysis applied in that study was claimed "to reproduce in general the polarity trend of $E_T(30)$ energies", this success may be rather ambiguous in view of the serious approximations involved.[62] Taking into account the red shift normally produced by dispersions, the higher value of Δ of the present analysis is not unexpected. The values $\hbar\omega_{abs} - \Delta G_p$ for some *n*-alkanes obtained from listed[3b] $E_T(30)$ energies and the δ parameters calculated by applying the $\Delta\alpha = 61$ Å^3 value are also shown in Figure 1b (open circles). Clearly, the strongly increasing dispersive solute−solvent interaction energies in the *n*-alkane series are inconsistent with invariable $E_T(30)$ values and with the analysis based on weakly polar fluids. On the other hand, the consistency of our analysis is supported by the good reproduction of the experimental absorption energies of aprotic liquids, not only those utilized in calculating $\Delta\alpha$ and Δ (see below).

For our further analysis we also need the ground state polarizability of the betaine-30 dye. In its absence we apply the Miller empirical method of additive atomic hybrid polarizabilities[63] giving $\alpha_0 = 68$ Å^3. This means a nearly doubling of the betaine-30 polarizability upon optical excitation rendering the effect of dispersions to be noticeable.

E. Dipolar Contribution. The spectral line shift produced by liquid (permanent and induced) dipoles is calculated here in the linear response approximation implying that the chemical potential of the solute dipolar solvation μ_p is proportional to the squared solute dipolar moment m_0: $\mu_p = m_0^2\mu^{(2)}$, where $\mu^{(2)}$ is the response function arising from the second-order perturbation expansion. Under this assumption, a very general determination of the absorption shift in terms of the high-frequency μ_p^∞ and inertial μ_p^{in} parts of μ_p is possible.[15d] In this way, the dipolar spectral shift is represented as the sum of two terms corresponding to the two separate time scales of the solvent: (i) the difference of the solvation chemical potentials $\Delta\mu^\infty$ of solvation by the fast electronic degrees of freedom and (ii) the work of changing the solute dipolar in the frozen reaction field Φ_{in}^g of the inertial solvent modes

$$\Delta E_p = \Delta\mu^\infty - \Delta m\Phi_{in}^g \qquad (16)$$

where Φ_{in}^g is related to the inertialess part of the solvation chemical potential by the expression

$$\Phi_{in}^g = -(\partial\mu_p^{in}/\partial m_0)|_{m_0 = m_g}$$

In order to get the shift, we need the response function $\mu^{(2)}$. We apply to this end the Padé form of the response function $\mu^{(2)}$ recently proposed by us[28b] as an extension of the Stell et al.[64a,b] theory of dipolar liquids and the Wertheim ansatz[64c] of incorporating the liquid polarizability. The latter replaces the polarizable liquid of coupled induced dipoles with a fictitious fluid with effective dipole moments calculated in a self-consistent manner. The Wertheim theory had been tested in molecular dynamics simulations[64d] and was found to be in excellent agreement with simulation data for the solvent dipole moments $\beta m^2/\sigma^3 < 3$, where m is the vacuum solvent dipole moment. The spectral shift stemming from differential solvation of ground, m_g, and excited, m_e, dipolar states of the solute is given by the relation[13b]

$$\Delta E_p = -\frac{2m'_g\Delta m}{\sigma^3}P - \frac{(m_e^\infty - m_g^\infty)\Delta m}{\sigma^3}P^\infty \qquad (17)$$

determined through the static $P = P(r_0,y,\eta)$ and high-frequency $P^\infty = P^\infty(r_0,y^\infty,\eta)$ Padé response functions depending on the reduced solute size $r_0 = R_0/\sigma + 1/2$, liquid-packing density η, and the dielectric parameters $y = (4\pi/9)\beta\rho m'^2 + (4\pi/3)\rho\alpha_s$ and

TABLE 2: Calculated (theor) and Observed (exp) Absorption Frequencies in 4-Nitroanisole and Betaine-30 Chromophores and Their Components Due to Induction Forces (ind), Permanent Dipole Solvation (perm), and Dispersion Interactions (disp) (All Energies in kcal/mol)

	π^*					$E_T(30)$				
solvent	ind	perm	disp	theor[d]	exp	ind	perm	disp	theor[d]	exp[a]
gas phase	0	0	0	103.5	105	0	0	0	37.45	
n-C_5[b]	−1.66	0	−1.95	99.23	98.26	1.05	0	−4.39	34.11	(31.00)
n-C_6[b]	−1.70	0	−2.22	99.62	98.00	1.06	0	−4.96	33.55	(31.00)
n-C_7[b]	−1.72	0	−2.45	99.38	97.92	1.06	0	−5.38	33.13	(31.10)
n-C_8[b]	−1.71	0	−2.75	99.08	97.66	1.04	0	−6.01	32.49	(31.10)
n-C_9[b]	−1.70	0	−2.96	98.87	97.58	1.03	0	−6.43	32.05	(31.00)
n-C_{10}[b]	−1.69	0	−3.15	99.70	97.46	1.02	0	−6.81	31.66	(31.00)
n-C_{11}[b]	−1.67	0	−3.45	98.42	97.41	1.00	0	−7.43	31.02	
n-C_{12}[b]	−1.64	0	−3.54	98.36	97.38	0.98	0	−7.63	30.80	(31.10)
PhH[c]	−2.47	0	−2.32	98.76	93.80	1.39	0	−4.77	34.07	34.30
PhMe[c]	−2.35	−0.11	−2.65	98.43	94.18	1.33	0.17	−5.50	33.46	33.90
m-xylene[c]	−2.27	−0.06	−2.96	98.30		1.28	0.10	−6.08	32.75	33.30
p-xylene[c]	−2.26	0	−3.09	98.32	94.43	1.28	0	−6.20	32.53	33.10
PhF[c]	−2.22	−2.11	−2.47	96.74	93.52	1.26	3.35	−5.13	36.93	37.00
PhCl[c]	−2.50	−2.21	−2.67	96.16	92.89	1.37	3.35	−5.35	36.81	36.80
PhBr[c]	−2.68	−2.22	−2.78	95.86	92.29	1.43	3.26	−5.44	36.70	36.60
PhI[c]	−2.85	−2.14	−2.86	95.69	91.77	1.50	3.06	−5.55	36.45	36.20
$PhNO_2$	−2.72	−6.27	−2.34	92.22	91.63	1.37	8.91	−4.32	43.41	41.20
PhCN	−2.58	−6.02	−2.86	92.09	91.55	1.36	9.13	−5.50	42.44	41.50
pyridine	−2.56	−4.30	−2.38	94.29	91.60	1.36	6.54	−4.65	40.70	40.50
CCl_4	−2.24	0	−2.02	99.28	96.12	1.30	0	−4.11	34.64	32.40
$CHCl_3$	−2.32	−1.16	−2.04	98.02	92.83	1.31	1.81	−4.05	36.52	39.10
CH_2Cl_2	−2.33	−3.08	−1.79	96.34	92.52	1.30	4.93	−3.55	40.14	40.70
1,1-DCE	−2.01	−3.34	−1.88	94.58		1.17	5.57	−3.995	40.19	39.40
1,2-DCE	−2.38	−3.25	−2.23	95.68	92.55	1.29	5.00	−4.31	39.43	41.300
1,1,2,2-TCE	−1.76	−1.39	−4.02	96.37	91.55	0.92	1.96	−7.48	32.86	
Me_2CO	−1.89	−4.97	−1.94	94.74	93.32	1.12	8.88	−4.15	43.30	42.20
MeCOEt	−1.93	−4.51	−1.89	95.21	93.43	1.13	7.78	−4.02	42.34	41.30
MeCOPr	−1.90	−4.04	−1.77	93.78		1.11	6.82	−4.89	40.49	41.10
MeCOBu	−1.91	−3.68	−1.64	93.98		1.11	6.07	−5.48	39.15	40.10
cyclohexanone	−2.28	−4.45	−2.85	93.97	92.86	1.22	6.74	−5.61	39.80	39.80
HCOOEt	−1.88	−2.76	−2.14	95.16		1.09	4.56	−4.52	38.58	40.90
MeOAc[c]	−1.90	−2.81	−2.29	96.54	94.20	1.09	4.60	−4.75	38.39	38.90
EtOAc	−1.88	−2.28	−2.41	96.96	94.43	1.10	3.75	−5.08	37.22	38.10
PrOAc	−1.84	−1.94	−2.61	95.75		1.08	3.15	−5.61	36.07	37.50
BuOAc	−1.83	−1.68	−2.81	95.90		1.07	2.70	−6.03	35.19	38.500
EtCN	−1.98	−5.84	−0.82	94.90	92.95	1.15	10.42	−1.68	47.34	43.60
n-PrCN	−2.00	−5.45	−1.47	94.61	92.89	1.15	9.28	−2.98	44.89	42.50
$MeNO_2$	−2.26	−6.93	−0.58	93.77	92.40	1.22	11.38	−1.13	48.92	46.30
$EtNO_2$	−2.95	−6.22	−0.53	93.84	92.26	1.62	10.37	−1.06	48.39	
cyclohexane[b]	−2.05	−0.01	−2.46	99.00	97.55	1.20	0.01	−5.17	33.49	
Et_3N[c]	−1.79	−0.24	−2.82	98.69	96.95	1.10	0.39	−6.68	32.26	32.10
Et_2O	−1.66	−1.14	−2.03	98.71	95.89	1.04	1.98	−4.61	35.86	34.50
THF[c]	−2.16	−2.81	−2.56	96.01	93.80	1.20	4.42	−5.20	37.87	37.40
HMPA	−2.11	−4.62	−2.49	94.32	91.57	1.21	7.37	−5.21	40.82	40.90
DMF	−2.42	−6.49	−1.53	93.10	91.49	1.27	10.01	−2.99	45.74	43.20
DMA	−1.91	−5.94	−2.86	92.83	91.75	1.01	9.08	−5.64	41.90	42.90
NMP	−2.45	−6.27	−2.28	92.54	91.26	1.24	9.04	−4.30	43.43	42.20
PC	−2.33	−7.09	−1.29	92.82	91.83	1.18	10.41	−2.26	46.79	46.00
DMSO	−2.65	−6.92	−1.34	92.63	90.69	1.34	10.21	−2.53	46.47	45.10
MeOH						1.13	7.70	−2.51	43.78	55.40
EtOH						1.17	5.81	−3.74	40.68	51.90
n-PrOH						1.16	4.62	−4.65	38.57	50.70
n-BuOH						1.17	3.76	−5.23	37.14	49.70
n-PeOH						1.14	3.17	−5.80	35.92	49.10
n-HeOH						1.12	2.66	−6.27	34.96	48.80
i-PrOH						1.16	4.55	−4.39	38.78	48.40
i-BuOH						1.18	3.76	−4.94	37.45	48.60
2-BuOH						1.16	3.75	−5.24	37.13	47.10
t-BuOH						1.15	3.71	−4.67	37.65	43.30
H_2O						1.18	11.55	−2.61	47.57	63.10

[a] The $E_T(30)$ values in parentheses are secondary quantities determined from a correlation relation with the data for the more lipophilic betaine-37 dye. [b] Nonpolar solvents used in determining $\Delta\alpha$ for 4-nitroanisole. [c] Solvents used in determining $\Delta\alpha$ for betaine-30. [d] The theoretical values are calculated without including the differential solvent component ΔE_{ss}.

$y^\infty = (4\pi/3)\rho\alpha_s$ of the liquid state solvent dipole moment m' and the polarizability α_s (the explicit relations for the Padé response functions P and P^∞ are given in Appendix B). The renormalized solvent dipole moment m' was calculated from its vacuum value in the framework of Wertheim theory.[64c] The solute dipole moments m_g and m_e are renormalized due to the static and high-frequency solvent responses and the nonzero solute polarizability α_0 to m'_g, m'_e and m_g^∞, m_e^∞ values, respectively. The vacuum solute dipole moment variation $\Delta m = m_e - m_g$ appears in eq 17 due to the positive energy of

TABLE 3: Dipolar Differential Solvation ΔE_p, Thermochromic Coefficients $Ts_{abs} = -T(\partial\hbar\omega_{abs}/\partial T)$, Differential Solvent Binding Energies ΔE_{ss}, and Deviations of the Theoretical Absorption Energies from Their Experimental Values (All Values in kcal/mol)

π^* scale[a]					$E_T(30)$ scale[b]				
solvent	$\Delta E_p/2$	$Ts_{abs}/2$	ΔE_{ss}	$\hbar\omega^{exp} - \hbar\omega^{th}$	solvent	$\Delta E_p/2$	$Ts_{abs}/2$	ΔE_{ss}	$\hbar\omega^{exp} - \hbar\omega^{th}$
n-C_5	−0.83	−2.45	−1.67	−1.67	PhH	−0.70	−2.15	1.45	0.23
n-C_6	−0.85	−2.27	−1.42	−1.61	PhMe	1.19	1.56	0.37	0.44
n-C_7	−0.86	−2.21	−1.35	−1.46	*p*-xylene	0.64	0.82	0.18	0.57
n-C_{12}	−0.82	−1.74	−0.92	−0.98	$CHCl_3$	1.56	8.62	7.06	2.88
cyclohexane	−1.03	−2.49	−1.46	−1.47	CH_2Cl_2	3.12	3.65	0.53	0.56
CCl_4	−1.12	−3.12	−2.0	−3.16	pyridine	3.95	3.72	−0.24	−0.20
PhH	−1.24	−3.77	−2.53	−4.96	DMA	5.05	3.80	−1.25	1.0
PhMe	−1.23	−3.14	−1.91	−4.25	$PhNO_2$	5.14	5.41	0.27	0.50
$CHCl_3$	−1.74	−3.38	−1.64	−5.19	PhCN	5.25	4.75	−0.50	−0.90
CH_2Cl_2	−2.71	−2.19	0.52	−3.23	DMF	5.64	3.40	−2.24	−2.54
					MeOH	4.41	5.14	0.73	11.62
					i-PrOH	2.86	5.63	2.77	9.62

[a] Experimental thermochromic coefficients are derived from data of ref 2b. [b] Experimental thermochromic coefficients are derived from the temperature variation of the shifts taken from refs 3c and 3e.

polarizing the solute which, as was also claimed by Luzhkov and Warshel,[65] amounts up to a half of the energy gain from solvent dipole stabilization. The two summands in eq 16 are given by

$$\Delta\mu^{\infty} = -(m_e^{\infty} + m_g^{\infty})\Delta m P^{\infty}/\sigma^3$$

and

$$\Phi_{in}^{g} = \frac{\Delta m}{\sigma^3}[2m'_g P - 2m_g^{\infty} P^{\infty}]$$

The dipolar shift of the fluorescence line can be obtained analogously to eq 17. The difference between the absorption and fluorescence energies is twice the reorganization energy. Its dipolar component $\lambda_{s,p}$ is given by the relation

$$\lambda_{s,p} = \frac{\Delta m}{\sigma^3}[\Delta m' P - \Delta m^{\infty} P^{\infty}] \qquad (18)$$

where $\Delta m^{\infty} = m_e^{\infty} - m_g^{\infty}$ and $\Delta m' = m'_e - m'_g$.

The ground and excited state solute dipole moments needed for calculating the dipolar part of solvent response are fairly well-known for both chromophores of interest. For the betaine-30 dye, the dipole moments $m_g = 14.8 \pm 1.2$ D and $m_e = 6.2 \pm 0.3$ D are reported.[3b] The dipole moments and polarizabilities (linear and quadratic) of 4-nitroanisole are well-established from both experimental[46,61,66] and calculation[48,67] techniques. The most accurate experimental methods of determining $m_{e,g}$ make use of electronic dichroism, electrical polarization of fluorescence, or Stark splitting of rotational spectra. We will accept here the values $m_g = 4.7$ D from dielectric measurements[61,66] and $m_e = 12.9$ D from electrochromism.[66] All the solute parameters used in the calculations are compiled in Table 1.

3. Results and Discussion

A. Solvent Polarity Dependence. It is usually held that the dispersion component is of subordinate importance[15b,39,65,68] for the solvent polarity dependence of optical spectral lines and that the solute−solvent induction forces are responsible for the spectral red shift[15b] in nonpolar solvents. In Table 2 we present the calculations of the solvent shifts in 4-nitroanisole and betaine-30 dissected into the contributions from inductions, permanent dipole orientations, and dispersion forces. As is seen, even for the relatively small 4-nitroanisole dye with little change in polarizability upon excitation, the dispersive part is comparable in magnitude to that of inductions. For the much larger betaine-30 dye, the induction effect is already totally overshadowed by the dispersions. Consequently, dispersion solvation may in no case be neglected in dealing with the red shift caused by a nonpolar solvent. This has already been suggested by DeBolt and Kollman[68] based on their inability to reproduce the red shift in CCl_4. It is further seen that in π^* the dipolar and dispersion components of the shift have the same sign and thus reinforce one another but counteract each other in $E_T(30)$.

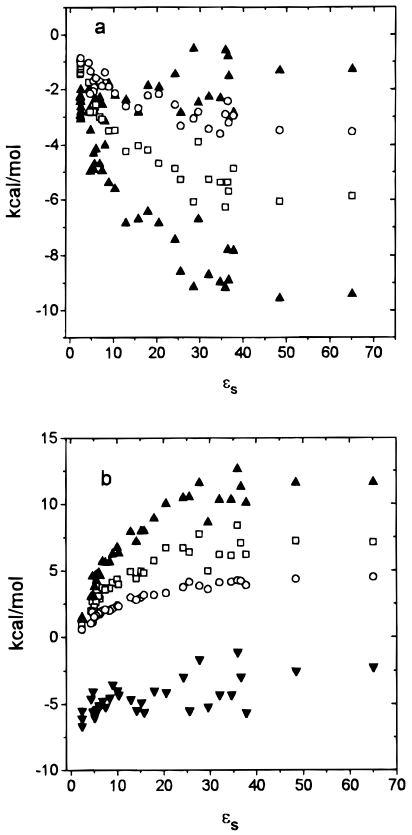

Figure 2. Dispersion (▼) and dipolar (▲) contribution to the UV−vis spectral solvent-induced shift in 4-nitroanisole (a) and betaine-30 (b) dyes. The open points exhibit the components of dipolar solvation due to permanent dipole reorientation (□) and local packing of the solvent around the solute (○).

In Figure 2 are shown the various contributions as a function of the dielectric constant addressing the long-standing issue regarding the trends occasionally observed between microscopic and macroscopic polarities. The dipolar solvation part changes more regularly with ϵ_s for betaine-30 than for 4-nitroanisole. This is primarily a size effect, since the continuum correlation $\propto (\epsilon_s - 1)/(2\epsilon_s + 1)$ is better obeyed the larger the chromophore.

By contrast, the dispersion part of the shift shows no particular trend with ϵ_s. Since in the π^* scale, however, the contribution of dispersion forces is small relative to the dipolar effect, correlations between π^* and ϵ_s within certain solvent classes become plausible.[5b] By the same token, the larger contribution of the dispersion part to the betaine-30 shift is the reason for the well-known fact that the observed $E_T(30)$ values cannot be expressed as functions of the dielectric constants.

Another interesting issue to address is the relative weighting of the orientational and packing contributions to the dipolar solvent strain produced by optical excitation. Since the reaction field of the inertial solvent modes Φ_{in}^g (eq 16) is not changed by optical transition, the excited configuration produces the state of strain for the nuclear solvent coordinates. This state is commonly attributed to nonequilibrium orientations of the solvent permanent dipoles to be changed in going to equilibrium. However, the solvent center-of-mass coordinates (local density) should also vary in the equilibration process and the state of strain should include the packing strain. In order to elucidate this point, in Figure 2 the total solvent response (including the inertial second term in eq 16 and the inertialess response of the induced dipole moments governed by the molecular coordinates distribution frozen on the transition time scale) is split into two constituent parts due to (i) orientational (permanent + induced dipoles) response[69] and (ii) correlations between the molecular coordinates (packing solvation).[13b,26b] The latter part amounts to about half the former thus making up about a third of the total ΔG_p. Just the same partitioning between the orientational and packing strains occurs in the terms $-\Delta m\Phi_{in}^g$ in eq 16.

Overall, the solvatochromic effect on the absorption energies of both chromophores is quite well-reproduced by our treatment as far as the nonpolar and select (aliphatic, aprotic, monofunctional) solvents are concerned (see Table 2 and Figure 3). For the π^* scale, the theoretical spectral energies $\Delta + \Delta E_{0s}$ are continuously higher than experimental values on the differential binding energy ΔE_{ss} (Figure 3a). The average difference for select solvents amounts to -1.6 kcal/mol. However, aromatic and halogenated solvents are anomalous. For these the calculated values are uniformly too high, pointing to the action of an additional solvation mechanism lowering the absorption energy (Figure 3a). This picture is reminiscent of the large body of linear solvation free energy relationships[5c,d] which deteriorate for the aromatic and halogenated solvents (in addition to the protic solvents, of course). As is well-known, an empirical remedy has been sought in terms of a "polarizability correction term". Likewise, in the relationships between the π^* scale and reaction field functions of the refractive index and the dielectric constant,[2e,6] the two solvent classes were found to constitute a special case. The additional solvating force can be sought in terms of solute−solvent π orbital overlap resulting in exciplex formation. As an example, weak solute−solvent complexes have actually been reported for aromatic solutes in CCl_4.[70] The sign of the theory−experiment deviation would tend to support the charge-transfer solvation mechanism. The solute excited state is generally more delocalized (Figure 4) and thus should be more receptive to solvation by solute−solvent overlap. The additional charge-transfer interaction would shift the line position to the red, as actually happens. In contrast to this, a variation in solute size induced by solute excitation (as suggested by Stratt and Adams[33a]) would shift the line to the blue which is not observed. Actually, blue shifts for positively solvatochromic dyes can be caused by the dominance of repulsions over attractions in the solvent response. This is possible indeed for solvents with very low LJ energies as for the benzene/He system in the experiments of Nowak and Bernstein.[32c] These

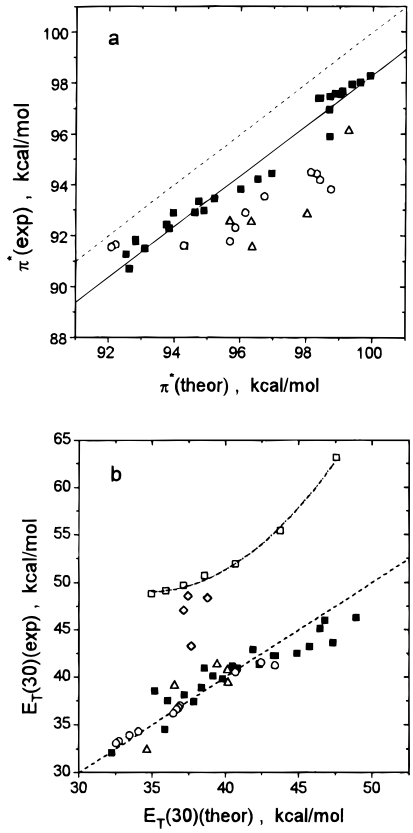

Figure 3. Experimental vs calculated absorption energies of 4-nitroanisole (a) and betaine-30 (b) for the solvent classes: (○) aromatics, (△) chlorinated, (□) *n*-alcohols, (◇) branched alcohols, and (■) others. The dashed line gives the identity between theory and experiment, the solid line in (a) is drawn through the select solvent points, and the dash−dotted line in (b) is drawn through the *n*-alcohols and water. The solute parameters used are listed in Table 1.

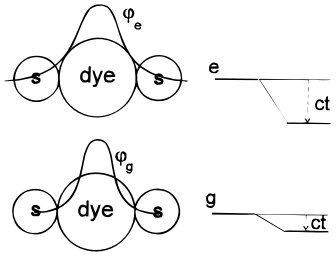

Figure 4. Schematic diagram of differential solvation by the solute(dye)−solvent(s) charge-transfer forces. ϕ_g and ϕ_e represent schematically the differing delocalization of the solute electronic density into the solvent region resulting in different lowering of the excited (e) and the ground (g) states.

conditions are not met for the highly polarizable solvents considered here. Therefore, assumption (2) of our calculation scheme might hold, whereas it is assumption (1) omitting the electronic overlap that accounts for our inability to reproduce the shift energies in solvents containing large polarizable chlorine atoms or aromatic orbitals.

In this context, it is instructive to compare our conclusions concerning the effect of specific forces on the π^* scale with a recent analysis by Horng et al.[71a] of the solvent-induced shifts in the coumarin 153 (C153) dye. The π^* scale, presumed to reflect only nonspecific solvent forces, has been employed in that study as the polarity indicator of spectral shifts. For the C153 chromophore, the aromatic solvents did not appear anomalous when viewed with the π^* polarity scale, but deviate significantly from the select solvents correlation in the Oshika−Baylis−McRae analysis.[15a,b] On the basis of the former

observation and on the arguably nonspecific character of the π^* indicator, the possibility of special complex formation has been rejected. Our present analysis, on the contrary, would suggest that the similarities in the effect of specific forces between the two (4-nitroanisole and C153) chromophores is the actual reason for the observed interrelation.

A possible effect of the solvent quadrupole moment may not be excluded in the attempt to rationalize the theory−experiment discord for the chlorinated and aromatic solvents.[71] The quadrupole and charge-transfer mechanisms reflecting, respectively, inertial and inertialess solvation pathways could be distinguished by a comparative analysis of absorption and fluorescence shifts. Unfortunately, for 4-nitroanisole fluorescence data are not available.

For $E_T(30)$, there is general agreement within ≃2 kcal/mol between experiment and theory for the bulk of the solvents (Figure 3b). In contrast to π^*, the chlorinated and aromatic solvents are well-behaved rendering assumption (1) to be adequate for this large chromophore. This comparison counts also in favor of the solute (e.g. charge transfer) instead of solvent (quadrupole moments) origin of the theory−experiment discord for these solvents in the case of 4-nitroanisole. The good behavior of the aromatic solvents could of course be attributed to the fact that they were used in determining $\Delta\alpha$ for betaine-30 (see Table 2). The value of $\Delta\alpha$ so obtained does not lead, however, to regular deviations from the theory for the solvents with small quadrupole moments. As is already shown in Figure 1b, the $E_T(30)$ values given for nonpolar solvents are at variance with our calculations. We obtain decreasing, instead of constant, $E_T(30)$ energies in the *n*-alkane series, caused by the strengthening of the dispersion coupling (see Table 2). We get for *n*-pentane, for instance, the value 34.11 kcal/mol, close to the experimental value 34.30 kcal/mol in benzene. This resemblance would seem reasonable in view of the very similar molecular properties (HS diameters, polarizabilities, and LJ energies) of the two solvents.

As is further seen in Figure 3b, the experimental $E_T(30)$ values for the H-bonding solvents are all considerably higher than our predictions. The origin of this divergence is not easy to assign unambiguously. Admittedly, the HS reference system implemented in the perturbation expansion, working well for nonpolar[72a,b] and dipolar[64] liquids, is no longer appropriate for H-bonding liquids[72c] because of the steep change of the attractive H-bonding forces with distance. Therefore, the HS distribution function may be a poor representation of the real solute−solvent correlations. As a result, the dispersion component of the absorption shift, most strongly affected by the choice of the reference pair distribution function, may be wrong. Anyway, the differences between theory and experiment are well above all conceivable errors made in calculating the dispersion component (Table 2). The solvent reorganization term not included in the calculations (Table 3) cannot account for the observed deviation. Another source of discrepancy may be attributed to solute−solvent hydrogen bonding not included in our calculation scheme (assumption (5)).[73] Actually, a larger blue shift compared to that produced by nonspecific forces is in agreement with previous studies of hydrogen-bonding effects on absorption spectra.[68,74] According to Haberfield's experiments,[74] the substantial part of the n → π^* shift of carbonyl dyes in going from dipolar aprotic to polar protic solvents is due to partial H-bond desolvation of the less polar excited state. This conclusion, general for hypsochromic shifts, was later supported by simulations of DeBolt and Kollman.[68] Consequently, the spectral shift of betaine-30 is an effective probe of solute−solvent hydrogen bonding which manifests itself also in solvation dynamics of the dye.[21c,d] Notice ultimately that the restriction to only the first multipole and the assumption of isotropic molecular polarizabilities (assumption (4)) does not seem to be very crucial to our analysis. These issues and possible uncertainties in the solvent molecular properties may account for the deviations in the 1−2 kcal/mol range of the calculated shifts from the presumably more exact spectroscopic data.

B. Differential Solvent Binding Energy. The values of the differential solvent binding energies calculated from eq 11 (the small solvent expansibility term has been omitted) are listed in Table 3. These are compared to the differences of experimental absorption energies $\hbar\omega^{exp}$ and the calculated values $\hbar\omega^{th} = \Delta + \Delta E_{0s}$ including only the solute−solvent internal energy variation. The first important conclusion from comparing Tables 2 and 3 is the small contribution of ΔE_{ss} relative to ΔE_{0s} for polar liquids. Thus a fairly accurate description can be achieved in this case in terms of only the solute−solvent component of the shift more easily amenable to a theoretical treatment. On the other hand, 4-nitroanisole has comparable ΔE_{0s} and ΔE_{ss} energies in nonpolar and weakly polar liquids. Although scattered, there is generally a good agreement between the ΔE_{ss} values from eq 11 and from the difference $\hbar\omega^{exp} - \hbar\omega^{th}$ for betaine-30 (excluding H-bonding solvents). This implies that the disregard of ΔE_{ss} in the $\Delta\alpha$ calculation above has not involved a considerable error. Concerning discrepancies between the two sets of values, they may originate from the errors of determining thermochromic coefficients s_{abs} which for some solvents have been calculated just for three temperatures.

An interesting feature coming to light in Table 3 is the opposite sign of ΔE_{ss} for the two dyes in nonpolar solvents. A qualitative understanding of the sign switch can be gained from the following reasoning. The optically induced increase in the solute dipole field enhances instantaneously the induced dipole moments of the solvent, thereby strengthening the solvent−solvent coupling in nonpolar liquids for a positively solvatochromic dye and vice versa. For polar solvents, on the other hand, the main contribution to the effective interaction potential variation ΔU_{ss} comes from the coupling of the solvent permanent dipoles to the increasing solute polarizability. The differential solvent binding should thus be negative in this case as actually seen in Table 3.

C. Solvent Reorganization Energy of ET. The evaluation of ET reorganization energies due to classical solvent and intramolecular solute modes is feasible by analyzing absorption band shapes. The customary procedure involves the assumption of two effective promoting modes, the one quantum-vibrational and the other classical, yielding the two corresponding reorganization energies, λ_v and λ_{cl}. A further subdivision of the classical component into solvent, λ_s, and classical vibrational, $\lambda_{cl,v}$, parts is, however, still rather ambiguous.[22b,21b] Solvent ET reorganization energy can, at least approximately, be extracted only for strongly polar fluids, for which continuum estimates work fairly well.[75] In weakly polar solvents, however, the continuum description is no longer correct. In this case it is usual practice to set the solvent ET reorganization energy equal to zero.[21b] Further, the classical intramolecular solute reorganization energy $\lambda_{cl,v}$ is assumed to be solvent independent and equal to that in nonpolar liquids. On the basis of this tentative assumption, the solvent component of the reorganization energy is then extracted. In light of this arbitrariness, the purpose of this section is 2-fold: (i) to calculate the solvent reorganization energy in order to reveal its contribution to λ_{cl} and (ii) to check the assumption of the solvent independence of $\lambda_{cl,v}$. Experimental data for λ_{cl} have been reported only for

TABLE 4: Classical Reorganization Energies of Betaine-30 (All Values in kcal/mol)

solvent	Q^a	$\lambda_{s,perm}{}^b$	$\lambda_{s,dens}{}^c$	$\lambda_{s,p}{}^d$	$\lambda_{s,c}{}^e$	$\lambda_{s,np}{}^f$	$\lambda_s{}^{th}$	$\lambda_{cl}{}^{exp,g}$	$\lambda_{cl,v}{}^h$
cyclohexane	0.042	0	0	0	0	0.06	0.06	4.77	4.71
PhH	0.654	0	0	0	0	0.04	0.04	5.44	5.40
PhMe	0.224	0.03	0.02	0.05	0.06	0.08	0.13	4.85	4.72
PhCN		1.61	1.04	2.65	0.96	0.38	3.03	8.60	5.57
Me_2CO	0.471	1.73	0.85	2.58	1.16	0.05	2.63	8.88	6.24
MeOAc	0.940	0.87	0.47	1.34	0.87	0.01	1.35	8.04	6.69
EtOAc		0.69	0.40	1.09	0.81	0.03	1.12	7.51	6.39

[a] Reduced quadrupole moments $Q^* = Q/(k_B T o^5)^{1/2}$ with quadrupole moments Q taken from ref 71b. [b] Calculated orientational component of solvent reorganization by the liquid permanent dipoles. [c] Calculated density component of solvent reorganization by the liquid permanent dipoles. [d] From eq 18. [e] From eq 19. [f] Calculated nonpolar solvent reorganization energy. [g] Experimental classical reorganization energy according to ref 21b. [h] Reorganization energy of the classical solute vibrations obtained as $\lambda_{cl,v} = \lambda_{cl}{}^{exp} - \lambda_s{}^{th}$.

betaine-30,[21b] shown in Table 4, where the total solvent ET reorganization energy is subdivided into the nonpolar contribution $\lambda_{s,npol}$ due to induction and dispersion forces and the polar part $\lambda_{s,p}$ produced by the liquid permanent dipoles (according to eq 18). Because of the relatively small ET dipole Δm on the one hand and the large size of betaine-30 on the other, the nonpolar part of the ET solvent reorganization energy is deemed to be of minor importance and may indeed be neglected for nonpolar solvents. The permanent dipole reorganization energy, $\lambda_{s,p}$, is subdivided in Table 4 into the component caused by the permanent dipole reorientations $\lambda_{s,perm}$ and dipolar translations $\lambda_{s,dens}$.[26b,69] The former stems from the one-dipole response and the dipolar correlations (orientational reorganization), and the latter (density reorganization) results from the center-of-mass correlations in the liquid. Taken together the nonpolar reorganization energy $\lambda_{s,npol}$ and the permanent dipoles translational part $\lambda_{s,dens}$ form the solvent reorganization energy by molecular translations $\lambda_{s,trans}$. As is seen, the dipolar density component amounts to about one-half of the orientational part of the permanent dipole reorganization energy, in accord with previous estimates for outersphere ET.[26b] The density component is thus an essential part of the solvent reorganization energy and can result in values of λ_s that even exceed the continuum estimates.[13b,26] The translational reorganization energy is generally lower than $\lambda_{s,perm}$ but in some cases as for benzonitrile in Table 4) may become close in magnitude to $\lambda_{s,perm}$.

The calculation results for $\lambda_{s,p}$ are compared in Table 4 to the continuum expression often used for intramolecular ET[22b,76a]

$$\lambda_{s,c} = \frac{\Delta m^2}{R_0{}^3}\left[\frac{\epsilon_s - 1}{2\epsilon_s + 1} - \frac{\epsilon_\infty - 1}{2\epsilon_\infty + 1}\right] \qquad (19)$$

where ϵ_∞ is the high-frequency solvent dielectric constant. As is seen in Table 4, the continuum values are generally smaller than $\lambda_{s,p}$ calculated from the molecular-based eq 18. The origin of this deviation is the solute polarizability enhancing the ET dipole moment Δm. This factor is thus important for bulky polarizable chromophores and should be included in λ_s calculations.

The comparison of Tables 2 and 4 shows that nonpolar solvation contributes considerably to the spectral shift, but affects far less the ET solvent reorganization energy. Thus, in ET terminology, dispersion and inductions are significant in the ET energy gap ΔG_{et} and may be disregarded in λ_s. This is opposite to the effect of dipolar forces contributing similarly to both values. The cause of this difference is rooted in different symmetries of isotropic (under the assumption of the isotropic molecular polarizability) dispersion and induction forces and anisotropic dipolar interactions. As a consequence, the energy gap contains the contribution from dispersions and inductions of the first order in the variation of the dispersion coupling $\Delta\alpha$ and the dipole moment $m_e{}^2 - m_g{}^2$, respectively. The reorganization energy due to dispersions and inductions is of the second order in $\Delta\alpha$ and $m_e{}^2 - m_g{}^2$ [13b] and thus is much smaller in magnitude. On the other hand, both the energy gap and the reorganization energy are quadratic in the ET dipole moment Δm for dipolar forces and are therefore of the same order. This distinction in the weightings of dispersions/inductions and dipolar forces in ΔG_{et} and λ_s may be responsible for the sometimes observed different solvent polarity variations of the two values.[76] Actually, for the charge separation reaction A−D $\rightarrow$ A^- − D^+, ΔG_{et} and λ_s should change in a similar way with solvent polarity,[77] provided the dispersion forces are excluded. For instance, in the continuum formulation of the outersphere charge separation reaction, the variation of the energy gap relative to some reference solvent

$$\delta\Delta G_{et} = \Delta G_{et}(\text{ref}) - \Delta G_{et}$$

is connected to λ_s by the simple relation

$$\kappa = \frac{\delta\Delta G_{et}}{\lambda_s} = \frac{1/\epsilon_{ref} - 1/\epsilon_s}{1/\epsilon_\infty - 1/\epsilon_s}$$

where ϵ_{ref} is the dielectric constant of the reference solvent. If a nonpolar solvent is chosen as the reference, κ should be close to unity. In contrast to this prediction, the results of the ET spectral shape analysis yield $\kappa = 0.47$[76b] in going from cyclohexane as the reference to chloroform.

For the $E_T(30)$ scale, the solvent reorganization energy is small relative to λ_{cl} for all solvents considered, pointing thus to a large contribution from the classical solute vibrations. The relatively small impact of the differential binding energy ΔE_{ss} on spectral shifts (Table 3) permits us to suggest that the term $\lambda_s{}^{(ss)}$ in eq 7 may hardly account for the obtained deviations. The appreciable solvent dependence of the classical vibrational reorganization energy $\lambda_{cl,v}$ is evident from Table 4. An appealing explanation of this feature is as follows. The vibrational reorganization energy $\lambda_{cl,v}$ can be solvent independent only if the promoting intramolecular vibrational mode is decoupled from the solvent polarization modes. The solvent dependence of $\lambda_{cl,v}$ is thus to be sought from intramolecular vibrations coupled to the solvent. Of these, the vibrations altering the donor−acceptor distance should be especially effective, since they modulate the solute electric field and consequently the equilibrium solvent polarization. Such molecular motions coupled with polarization fluctuations actually produce an additional component of the solvent reorganization energy with solvent polarity and intramolecular vibration properties mixed.[78] If the donor and acceptor moieties vibrate against one another with the classical frequency ω, $\hbar\omega < 2k_BT$ about the equilibrium distance R_{ad}, the classical reorganization energy of intramolecular ET attains, in a continuum solvent description, the form[78a,b]

$$\lambda_{el} = \lambda_s + \left(1 - \frac{1}{\epsilon_s}\right)^2 \frac{\Delta m^2 e^2}{9E_v R_0^4} + \sum_j \lambda_{cl,v}(j) \qquad (20)$$

where $E_v = {}^1/_2 f_{ad} R_{ad}^2$, $f_{ad} = M\omega^2$, M is the reduced donor−acceptor mass, and e is the electron charge. The summation in the last term of eq 20 is over the classical intramolecular vibrations of the solute including the donor−acceptor mode. Since the classical donor−acceptor vibration provides an inertial mode changing the effective energy difference ΔE_{0s} (eq 1), the second mixture term is nonzero even for nonpolar liquids displaying the solvent dependence $\propto (1 - 1/\epsilon_s)^2 \Delta m'^2/R_0^6$. In the present molecular treatment, the solute dipole moments m_g' and m_e' and the effective solute radius R_0 are solvent dependent. The latter feature is, however, inconsistent with the continuum approach utilized in deriving eq 20. A more detailed analysis of the vibration−polarization coupling will be presented elsewhere.[78c] For the present analysis, the continuum reorganization energy $\lambda_{s,c}$ is more consistent with eq 20. The difference of λ_{cl}^{exp} and $\lambda_{s,c}$ actually demonstrates a linear trend with $(1 - 1/\epsilon_s)^2$ as shown in Figure 5. To provide such a solvent variation the donor−acceptor vibrational mode should be soft enough with $f_{ad} \simeq 0.01$ eV/Å^2.

An alternative explanation of the deviation between λ_s^{exp} and λ_s^{th} in Table 4 may be sought in terms of solvation by higher solvent multipoles (e.g. quadrupoles) not included in λ_s^{th} and claimed to be an important contribution to ET solvent reorganization at low solvent polarities.[41,71b] A trend between $\lambda_s^{exp} - \lambda_s^{th}$ and the reduced solvent quadrupole moment $Q^* = Q/(k_B T\sigma^5)^{1/2}$ is actually seen in Figure 6. No definite conclusion can be drawn from this correlation, and further studies on this problem are certainly required. Just note that the effect of higher multipoles is expected to be of subordinate importance to dipolar reorganization for polar solvents like acetone. The difference $\lambda_s^{exp} - \lambda_s^{th}$ is, however, higher than $\lambda_{s,p}$ itself and can thus hardly be attributed to solvation by higher solvent multipoles.

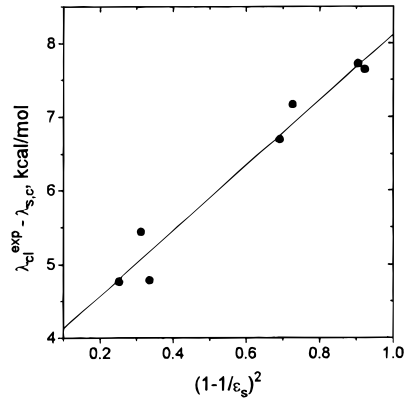

Figure 5. Variation of the reorganization energy of the solute classical vibrations $\lambda_{cl}^{exp} - \lambda_{s,c}$ obtained in the continuum model vs the polarity factor $(1 - 1/\epsilon_s)^2$ for the solvents (●) from Table 4. The solid line displays the regression with the slope 4.43 kcal/mol.

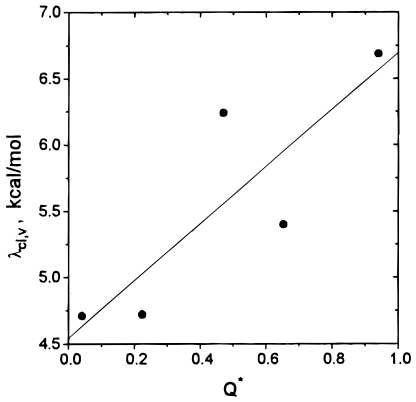

Figure 6. The difference $\lambda_{cl}^{exp} - \lambda_s^{th}$ vs reduced quadrupole moments $Q^* = Q/(k_B T\sigma^5)^{1/2}$ for the solvents (●) from Table 4. The solid regression line is drawn as a guide for the eye.

4. Summary

The effects of nonspecific long-range forces on the spectral shifts in the dyes 4-nitroanisole and betaine-30 forming the basis of the π^* and $E_T(30)$ polarity scales, respectively, have been calculated at a molecular level. For the nonpolar and select solvents the shift values are reproduced reasonably well, for both dyes, with experiment/theory deviations of about 1−2 kcal/mol. This testifies to the contention that the solute−solvent interactions probed by these dyes are in general long-ranged. We are thus able to elucidate some general features of optical shifts in molecular fluids, summarized as follows, according to the issues addressed in the Introduction.

(1) We have quantified the contributions of induction, dispersion, and dipole−dipole long-range solute−solvent forces to the spectral shifts. Solvatochromism has its origin in the changes in polarizability and dipole moment of the dye upon electronic excitation provoking differential solvation of the ground and excited states. Both these solute parameters are claimed here to be indispensable to a realistic spectral shift analysis. The solvent response to transition dipole creation is of composite nature incorporating self-consistently the effects of (i) molecular polarizability, (ii) permanent dipole orientation, and (iii) packing constraints about the solute. Since all these three factors are not amenable to full decoupling, we studied the relative effects of (i) and (iii). In Table 2, the dipolar response is subdivided into the effects of polarizability and permanent dipoles. The former component has been extracted by setting the solvent permanent dipoles equal to zero. The high-frequency induction component is always an appreciable part of the dipolar response. The extraction of the orientational (permanent + induced dipoles) dipolar response is performed by switching off the center-of-mass correlations in the liquid. This projects out roughly one-third of the effect of packing constraints in the dipolar solvent response (Figure 2). Hence, although the orientation of permanent dipoles (point (ii) above) remains the key contributor to the solvent effect in strongly polar liquids, the other two effects are not marginal.

An important result of this work is emphasizing the importance of dispersion forces, also in highly polar liquids. Controlled by solute polarization enhancement upon excitation, dispersion forces are strongly dependent on solute size. Thus, while dispersion and induction are comparable in magnitude in π^*, induction is clearly overshadowed by dispersion in $E_T(30)$. Furthermore, both effects have the same direction in π^*, producing the well-known red shift. For $E_T(30)$, dispersion and induction forces counteract each other making the red shift peculiar to nonpolar solvents switch to the blue for polar solvents. Betaine-30 provides thus experimental verification of our previous contention[13a] that the shift may switch upon transfer through solvents due to the opposite sign of the dispersion and dipolar forces effects. Another example of such a behavior is the negatively solvatochromic stilbazolium betaine dye long believed to be capable of the solvatochromism switch.[79] There was no need to include an alteration of the solute effective size with optical excitation for the two dyes considered.

(2) By comparing the theoretical and experimental shifts, the role played by specific solute−solvent forces can be assessed.

The interpretation is made easier in terms of solvent classes. Thus, the chlorinated and aromatic solvents have a stronger effect on the shift of 4-nitroanisole than would be expected solely from the long-range forces considered. The neglected solvation power can be identified with charge transfer between solute and solvent. Since in the case of betaine-30 the solvent classes noted are not exceptional, charge-transfer effects may be surmised to become prominent only for small dyes of delocalized electronic density. For betaine-30, on the other hand, the theoretical shifts in H-bonding solvents are considerably below experiment giving an estimate of about 10 kcal/mol difference between solute−solvent H-bonding in the ground and excited states. Notice thus the opposite sign of the theory/experiment deviations for the two dyes: charge-transfer interactions stabilize the state of higher delocalization, i.e. the excited state of 4-nitroanisole; H-bonding interactions stabilize the solute state with the higher dipole moment which is the ground state for betaine-30.

(3) Differential solvent binding energies contribute additively to the solvent-induced spectral shift and ET reorganization energy. These arise from the instantaneous variation of the solvent−solvent interaction in the course of optical transition rooted in molecular polarizability effects. The solvent−solvent part of the spectral shift ΔE_{ss} has been evaluated from experimental thermochromic data and was found to be small relative to the solute−solvent contribution in polar liquids. In weakly polar and nonpolar solvents, the two parts may be of comparable magnitudes (cf. Tables 2 and 3 for 4-nitroanisole). For nonpolar liquids, ΔE_{ss} switches its sign from negative for positively solvatochromic dyes to positive for negatively solvatochromic chromophores. For polar liquids, ΔE_{ss} is always negative.

Acknowledgment. This work has been partially supported by Grant No. CHE-9520619 from the National Science Foundation. We thank Prof. M. Newton for sending us a preprint of ref 40.

Appendix A

As a result of the averaging over the solvent high-frequency modes, both the solute−solvent and solvent−solvent interaction potentials in eq 1 become state dependent. In this Appendix, we give a proof to this statement for a model system of a polarizable dipolar solute in the solvent of polarizable dipolar spheres bearing permanent dipoles m and possessing the polarizability α. Optical excitation of the solute is assumed to result in the variation of the permanent dipole moment $\mathbf{m}_0^{(1)} \rightarrow \mathbf{m}_0^{(2)}$ and the polarizability $\alpha_0^{(1)} \rightarrow \alpha_0^{(2)}$, where "0" refers to the solute. The system Hamiltonian can be considered as a sum of the solute $H_0^{(i)}$, solvent H_s, and interaction $H_{0s}^{(i)}$ parts

$$H^{(i)} = H_0^{(i)} + H_{0s}^{(i)} + H_s$$

The solvent Hamiltonian involves the dipole−dipole interaction between the permanent $\mathbf{m}_j$ and induced $\mathbf{p}_j$ dipoles located at the jth molecule ($\mathbf{T}_{jk}$ is the dipolar tensor)

$$H_s = -{}^1/_2\sum_{j\neq k}(\mathbf{m}_j + \mathbf{p}_j)\cdot\mathbf{T}_{jk}\cdot(\mathbf{m}_k + \mathbf{p}_k) + \sum_j H_0(\mathbf{p}_j)$$

and the intermolecular solvent Hamiltonians $H_0(\mathbf{p}_j)$ describing the internal dynamics resulting in molecular polarizability. We will model $H_0(\mathbf{p}_j)$ in the static Drude oscillator form

$$H_0(\mathbf{p}_j) = \mathbf{p}_j^2/(2\alpha)$$

thus disregarding the frequency dependence of α and consequently the dispersion forces. An analogous form is taken for the solute-induced dipole $\mathbf{p}_0$

$$H_0^{(i)}(\mathbf{p}_0) = \mathbf{p}_0^2/(2\alpha_0^{(i)})$$

The solute−solvent interaction Hamiltonian has the form

$$H_{0s}^{(i)} = -\mathbf{m}_0^{(i)}\cdot\sum_j \mathbf{T}_{0j}\cdot(\mathbf{m}_j + \mathbf{p}_j)$$

The energetic states of the solute probed by optical excitations are equilibrated to the inertialess solute and solvent polarizabilities and thus can be obtained from the partial partition functions

$$\exp[-\beta U^{(i)}] = \int \exp[-\beta H^{(i)}]\, d\mathbf{p}_0 \prod_j d\mathbf{p}_j$$

For the Drude harmonic oscillator model this integration can be easily performed yielding

$$U^{(i)} = U_{0s}^{(i)} + U_{ss}^{(i)}$$

The state dependent solute−solvent interaction potential is given by

$$U_{0s}^{(i)} = -\mathbf{m}_0^{(i)}\cdot\sum_j [\mathbf{T}_{0j} + \alpha\mathbf{T}_{0n}\cdot(\boldsymbol{\pi}_{nk}^{(i)})^{-1}\cdot(\mathbf{T}_{kj} + \alpha_0^{(i)}\mathbf{T}_{k0}\cdot\mathbf{T}_{0j})]\cdot\mathbf{m}_j \quad \text{(A1)}$$

where

$$\boldsymbol{\pi}_{jk}^{(i)} = \delta_{jk} - \alpha\mathbf{T}_{jk} - \alpha_0^{(i)}\mathbf{T}_{j0}\cdot\mathbf{T}_{0k}$$

The solvent−solvent interaction potential also gains the dependence on the solute state

$$\begin{aligned} U_{ss} = &-({}^1/_2)\sum_{j\neq k}\mathbf{m}_j\cdot\mathbf{T}_{jk}\cdot\mathbf{m}_k - \\ &(\alpha_0^{(i)}/2)\sum_{j\neq k}\mathbf{m}_j\cdot\mathbf{T}_{j0}\cdot\mathbf{T}_{0n}(\delta_{nk} + 2\alpha(\boldsymbol{\pi}_{nm}^{(i)})^{-1}\cdot\mathbf{T}_{mk})\cdot\mathbf{m}_k - \\ &(\alpha/2)\sum_{j\neq k}\mathbf{m}_j\cdot\mathbf{T}_{jm}\cdot(\boldsymbol{\pi}_{mn}^{(i)})^{-1}\cdot\mathbf{T}_{nk}\cdot\mathbf{m}_k - \\ &(\alpha\alpha_0^{(i)2}/2)\sum_{j\neq k}\mathbf{m}_j\cdot\mathbf{T}_{j0}\cdot\mathbf{T}_{0m}\cdot(\boldsymbol{\pi}_{mn}^{(i)})^{-1}\cdot\mathbf{T}_{n0}\cdot\mathbf{T}_{0k}\cdot\mathbf{m}_k \end{aligned} \quad \text{(A2)}$$

Eq A2 looks rather complicated, but the main state dependent term for polar fluids is

$$(\alpha_0^{(i)}/2)\sum_{j\neq k}\mathbf{m}_j\cdot\mathbf{T}_{j0}\cdot\mathbf{T}_{0k}\cdot\mathbf{m}_k \quad \text{(A3)}$$

implicating the coupling of the solvent permanent dipole through the state dependent solute induced dipole. This additional solvent−solvent coupling decays as $\propto 1/r_{0j}^3 r_{0k}^3$ with the solute−solvent distance and due to the large solute polarizability $\alpha_0^{(i)}$ may noticeably modify the solvent−solvent interaction in the solute vicinity. The variation of the solvent−solvent coupling ΔU_{ss} should thus be proportional to the change of the solute polarizability $\Delta\alpha$.

Appendix B

The Padé functions of the solvent linear response to dipole solvation are given[28b] in the form factoring the density and polarity dependencies as follows

TABLE 5: Coefficients of the Density Expansion of the Functions $a(\rho^*)$, $b(\rho^*)$, and $c(\rho^*)$ in the Integral $I_{0s}^{(3)}$ and $d(\rho^*)$, and $f(\rho^*)$ in $I_{0s}^{(2)}$

i	a	b	c	d	e	f
0	1	−9/16	1/32	0	0	0
1	0.6024	0.2547	−0.2562	1.9350	−1.675	0.4390
2	−0.3808	0.8483	−0.2632	−0.9721	2.183	−1.0510
3	−0.0611	−0.1072	−0.0983	0.3982	−0.8311	0.4653

$$P(y,\rho^*,r_0) = \frac{yI_{0s}^{(2)}}{1 + yI_{0s}^{(3)}/I_{0s}^{(2)}}$$

where $I_{0s}^{(2)}$ and $I_{0s}^{(3)}$, respectively, are two- and three-particle solute−solvent integrals. They have been represented by simple polynomials of the reduced solvent density $\rho^* = \rho\sigma^3$ and r_0

$$I_{0s}^{(2)} = \frac{a(\rho^*)}{r_0^3} + \frac{b(\rho^*)}{r_0^4} + \frac{c(\rho^*)}{r_0^6}$$

$$I_{0s}^{(3)} = \frac{1}{r_0^3} + \frac{d(\rho^*)}{r_0^4} + \frac{e(\rho^*)}{r_0^5} + \frac{f(\rho^*)}{r_0^6}$$

where $a(\rho^*)$, $b(\rho^*)$, $c(\rho^*)$, $d(\rho^*)$, and $e(\rho^*)$ are the third-order polynomials of ρ^* as, for instance,

$$a(\rho^*) = a_0 + a_1\rho^* + a_2\rho^{*2} + a_3\rho^{*3}$$

The polynomial coefficients listed in Table 5 have been fitted to the calculated ρ^* and r_0 dependencies of $I_{0s}^{(2)}$ and $I_{0s}^{(3)}$.

References and Notes

(1) (a) Marcus, Y. *Ion Solvation*; Wiley, Chichester, U.K. 1985. (b) Marcus, Y. *Chem. Soc. Rev.* **1993**, *22*, 409.

(2) (a) Kamlet, M. J.; Abboud, J.-L. M.; Taft, R. W. *J. Am. Chem. Soc.* **1977**, *99*, 6027. (b) Nicolet, P.; Laurence, C. *J. Chem. Soc., Perkin Trans. 2* **1986**, 1071. (c) Brady, J. E.; Carr, P. W. *J. Phys. Chem.* **1985**, *89*, 1813. (d) Bekárek, V.; Bekárek, Š.; Pavlát, F. *Z. Phys. Chem. (Leipzig)* **1988**, *269*, 1147. (e) Bekárek, V. *J. Phys. Chem.* **1981**, *85*, 722.

(3) (a) Reichardt, C. *Chem. Soc. Rev.* **1992**, *21*, 147. (b) Reichardt, C. *Chem. Rev.* **1994**, *94*, 2319. (c) Laurence, C.; Nicolet, P.; Reichardt, C. *Bull. Soc. Chim. Fr.* **1987**, 125. (d) Reichardt, C.; Harbusch-Görnert, E. *Liebigs Ann. Chem.* **1983**, 721. (e) Linert, W.; Jameson, R. F. *J. Chem. Soc., Perkin Trans. 2*, 1415.

(4) Kamlet, M. J.; Abboud, J.-L.; Taft, R. W. *Prog. Phys. Org. Chem.* **1981**, *13*, 485.

(5) (a) Taft, R. W.; Murray, J. S. In *Quantitative Treatment of Solute-Solvent Interactions*; Politzer, P., Murray, J. S., Eds.; Elsevier: Amsterdam, 1994. (b) Abboud, J.-L.; Taft, R. W.; Kamlet, M. J. *J. Chem. Res. (S)* **1984**, 98. (c) Kamlet, M. J.; Abboud, J.-L. M.; Abraham, M. H.; Taft, R. W. *J. Org. Chem.* **1983**, *48*, 2877. (d) Taft, R. W.; Abboud, J.-L. M.; Kamlet, M. J. *J. Am. Chem. Soc.* **1981**, *103*, 1080.

(6) Laurence, C.; Nicolet, P.; Dalati, M. T.; Abboud, J.-L. M.; Notario, R. *J. Phys. Chem.* **1994**, *98*, 5807.

(7) The π^*-scale was originally constructed by averaging the UV−vis spectral shift data for several (seven[2a]) indicators. This way of proceeding looses some important physical details and is not acceptable from the viewpoint of molecular-based calculations sensitive to the solute size, dipole moment, polarizability, etc. A scale based on data for a single indicator is preferable, and 4-nitroanisole was suggested[6] as such a molecular probe.

(8) If a molecule possesses an anisotropic polarizability, orientational fluctuations would also contribute to dispersion and induction forces effects, but density fluctuations are expected to be more important.

(9) Giesen, D. J.; Storer, J. W.; Cramer, C. J.; Truhlar, D. G. *J. Am. Chem. Soc.* **1995**, *117*, 1057. (b) Amovilli, C. *Chem. Phys. Lett.* **1994**, *229*, 244.

(10) (a) Harder, T.; Bendig, J. *Chem. Phys. Lett.* **1994**, *228*, 621. (b) Andersson, P. O.; Gillbro, T.; Ferguson, L.; Cogdell, R. J. *Photochem. Photobiol.* **1991**, *54*, 353.

(11) (a) Rauhut, G.; Clark, T.; Steinke, T. *J. Am. Chem. Soc.* **1993**, *115*, 9174. (b) Leontidis, E.; Suter, U. W.; Schütz, M.; Lüthi, H.-P.; Renn, A.; Wild, U. P. *J. Am. Chem. Soc.* **1995**, *117*, 7493.

(12) (a) Fourkas, J. T.; Berg, M. *J. Chem. Phys.* **1993**, *98*, 7773. (b) Ma, J.; Bout, D. V.; Berg, M. *J. Chem. Phys.* **1995**, *103*, 9146. (c) Ladanyi, B. M.; Stratt, R. *J. Phys. Chem.* **1996**, *100*, 1266.

(13) (a) Matyushov, D. V.; Schmid, R. *J. Chem. Phys.* **1995**, *103*, 2034. (b) Matyushov, D. *Chem. Phys.*, in press.

(14) (a) Sánchez, M. L.; Aguilar, M. A.; Olivares del Valle, F. J. *J. Phys. Chem.* **1995**, *99*, 15758. (b) Mikkelsen, K. V.; Cesar, A.; Ågren, H.; Jensen, H. J. A. *J. Chem. Phys.* **1995**, *103*, 9010.

(15) (a) Oshika, Y. *J. Phys. Soc. Jpn.* **1954**, *9*, 594. (b) Bayliss, N. S.; McRae, E. G. *J. Phys. Chem.* **1954**, *58*, 1002. (c) Mataga, N.; Kaifu, Y.; Koizumi, M. *Bull. Chem. Soc. Jpn.* **1956**, *29*, 456. (d) Liptay, W. *Z. Naturforsch.* **1965**, *20a*, 1441.

(16) (a) van der Zwan, G.; Hynes, J. T. *J. Phys. Chem.* **1985**, *89*, 4181. (b) Fonseca, T.; Ladanyi, B. M.; Hynes, J. T. *J. Phys. Chem.* **1992**, *96*, 4085.

(17) (a) Garisto, F.; Kusalik, P. G.; Patey, G. N. *J. Chem. Phys.* **1983**, *79*, 6294. (b) Yu, H.-A.; Karplus, M. *J. Chem. Phys.* **1988**, *89*, 2366. (c) Yu, H.-A.; Roux, B.; Karplus, M. *J. Chem. Phys.* **1990**, *92*, 5020.

(18) (a) Franck, H. S.; Evans, M. W. *J. Chem. Phys.* **1945**, *13*, 507. (b) Pangali, C.; Rao, M.; Berne, B. J. *J. Chem. Phys.* **1979**, *71*, 2982. (c) Zichi, D. A.; Rosski, P. J. *J. Chem. Phys.* **1985**, *83*, 797. (d) Matubayasi, N. *J. Am. Chem. Soc.* **1994**, *116*, 1450. (e) Matubayasi, N.; Reed, L. H.; Levy, R. M. *J. Phys. Chem.* **1994**, *98*, 10640.

(19) Grunwald, E.; Steel, C. *J. Am. Chem. Soc.* **1995**, *117*, 5687.

(20) (a) Marcus, R. A. *J. Chem. Phys.* **1956**, *24*, 966. (b) Marcus, R. A. *Rev. Mod. Phys.* **1993**, *65*, 599.

(21) (a) Åkesson, E.; Walker, G. C.; Barbara, P. F. *J. Chem. Phys.* **1991**, *95*, 4188. (b) Walker, G. C.; Åkesson, E.; Johnson, A. E.; Levinger, N. E.; Barbara, P. F. *J. Phys. Chem.* **1992**, *96*, 3728. (c) Reid, P. J.; Alex, S.; Jarzeba, W.; Schlief, R. E.; Johnson, A. E.; Barbara, P. F. *Chem. Phys. Lett.* **1994**, *229*, 93. (d) Reid, P. J.; Barbara, P. F. *J. Phys. Chem.* **1995**, *99*, 3554.

(22) (a) Kjaer, A. M.; Ulstrup, J. *J. Am. Chem. Soc.* **1987**, *109*, 1934. (b) Cortés, J.; Heitele, H.; Jortner, J. *J. Phys. Chem.* **1994**, *98*, 2527.

(23) (a) Ma, J.; Dutt, G. B.; Waldeck, D. H.; Zimmt, M. B. *J. Am. Chem. Soc.* **1994**, *116*, 10619. (b) Morais, J.; Zimmt, M. B. *J. Phys. Chem.* **1995**, *99*, 8863. (c) Tepper, R. J.; Zimmt, M. B. *Chem. Phys. Lett.* **1995**, *241*, 566.

(24) (a) Markel, F.; Ferris, N. S.; Gould, I. R.; Myers, A. B. *J. Am. Chem. Soc.* **1992**, *114*, 6208. (b) Kulinowski, K.; Gould, I. R.; Myers, A. B. *J. Phys. Chem.* **1995**, *99*, 9017.

(25) Britt, B. M.; McHale, J. L.; Friedrich, D. M. *J. Phys. Chem.* **1995**, *99*, 6347.

(26) (a) Matyushov, D. V. *Mol. Phys.* **1993**, *79*, 795. (b) Matyushov, D. V. *Chem. Phys.* **1993**, *174*, 199.

(27) (a) Maroncelli, M. *J. Chem. Phys.* **1991**, *94*, 2084. (b) Perera, L.; Berkowitz, M. L. *J. Chem. Phys.* **1992**, *96*, 3092.

(28) (a) Matyushov, D.; Schmid, R. *J. Chem. Phys.* **1996**, *104*, 8627. (b) Matyushov, D. V.; Schmid, R. *J. Chem. Phys.* **1996**, *105*, 4729.

(29) Baer, S. *J. Chem. Phys.* **1974**, *60*, 435.

(30) (a) Thompson, M. J.; Schweizer, K. S.; Chandler, D. *J. Chem. Phys.* **1982**, *76*, 1128. (b) Chandler, D.; Schweizer, K. S.; Wolynes, P. G. *Phys. Rev. Lett.* **1982**, *49*, 1100. (c) Schweizer, K. S. *J. Chem. Phys.* **1986**, *85*, 4638.

(31) (a) Warshel, A. *J. Phys. Chem.* **1982**, *86*, 2218. (b) Tachiya, M. *J. Phys. Chem.* **1989**, *93*, 7050.

(32) (a) Saxton, M. J.; Deutch, J. M. *J. Chem. Phys.* **1974**, *60*, 2800. (b) Messing, I.; Raz, B.; Jortner, J. *J. Chem. Phys.* **1977**, *66*, 2239. (c) Nowak, R.; Bernstein, E. R. *J. Chem. Phys.* **1987**, *87*, 2457. (d) Heidenreich, A.; Bahatt, B.; Ben-Norin, N.; Even, U.; Jortner, J. *J. Chem. Phys.* **1994**, *100*, 6300.

(33) (a) Stratt, R. M.; Adams, J. E. *J. Chem. Phys.* **1993**, *99*, 775. (b) Adams, J. E.; Stratt, R. M. *J. Chem. Phys.* **1993**, *99*, 789. (c) Bader, J. S.; Berne, B. J. *J. Chem. Phys.* **1996**, *104*, 1293.

(34) Roux, R.; Yu, H.-A.; Karplus, M. *J. Phys. Chem.* **1990**, *94*, 4683.

(35) (a) Luque, F. J.; Bofill, J. M.; Orozco, M. *J. Chem. Phys.* **1995**, *103*, 10183. (b) Gao, J.; Habibollazadeh, D.; Shao, L. *J. Phys. Chem.* **1995**, *99*, 16460. (c) Meng, E. C.; Caldwell, J. W.; Kollman, P. A. *J. Phys. Chem.* **1996**, *100*, 2367.

(36) (a) Burshulaya, B. D.; Zichi, D. A.; Kim, H. J. *J. Phys. Chem.* **1995**, *99*, 10069. (b) Kumar, P. V.; Maroncelli, M. *J. Chem. Phys.* **1995**, *103*, 3038. (c) Horng, M. L.; Gardecki, J. A.; Papazyan, A.; Maroncelli, M. *J. Phys. Chem.* **1995**, *99*, 17311.

(37) (a) Klopman, G. *Chem. Phys. Lett.* **1967**, *1*, 200. (b) Germer, H. *Theor. Chim. Acta* **1974**, *35*, 273.

(38) Cramer, C. J.; Truhlar, D. G. *J. Am. Chem. Soc.* **1991**, *113*, 8305.

(39) (a) Zeng, J.; Craw, J. S.; Hush, N. S.; Reimers, J. R. *J. Chem. Phys.* **1993**, *99*, 1482; *Ibid.* **1993**, *99*, 1496. (b) Zeng, J.; Craw, J. S.; Hush, N. S.; Reimers, J. R. *J. Chem. Phys.* **1994**, *98*, 11075; **1995**, *99*, 10459. (c) Zeng, J.; Craw, J. S.; Hush, N. S.; Reimers, J. R. *J. Am. Chem. Soc.* **1995**, *117*, 8618.

(40) (a) Reineri, F. O.; Zhou, Y.; Friedman, H. L.; Stell, G. *Chem. Phys.* **1991**, *152*, 201. (b) Chong, S.-H.; Miura, S.; Basu, G.; Hirata, F. *J. Phys. Chem.* **1995**, *99*, 10526.

(41) Perng, B.-C.; Newton, M.; Raineri, F. O.; Friedman, H. L. *J. Chem. Phys.* **1996**, *104*, 7177.

(42) (a) Boublik, T. *J. Chem. Phys.* **1970**, *53*, 471. (b) Mansoori, G. A.; Carnahan, N. F.; Starling, K. E.; Leland, T. W., Jr. *J. Chem. Phys.* **1971**, *54*, 1523.

(43) (a) Ben-Amotz, D. *J. Phys. Chem.* **1993**, *97*, 2319. (b) Souza, L. E. S.; Stamatopoulou, A.; Ben-Amotz, D. *J. Chem. Phys.* **1994**, *100*, 1456. (c) Souza, L. E. S.; Ben-Amotz, D. *J. Chem. Phys.* **1994**, *101*, 9858.

(44) Ravi, R.; Souza, L. E. S.; Ben-Amotz, D. *J. Phys. Chem.* **1993**, *97*, 11835.

(45) (a) Reiss, H. *Adv. Chem. Phys.* **1965**, *1*, 9. (b) Boublik, T. *Mol. Phys.* **1974**, *27*, 1415.

(46) Paley, M. S.; Harris, J. M.; Looser, H.; Baumert, J. C.; Bjorklund, G. C.; Jundt, D.; Twieg, R. J. *J. Org. Chem.* **1989**, *54*, 3774.

(47) (a) Kromhout, R. A.; Linder, B. *J. Phys. Chem.* **1995**, *99*, 16909. (b) Vieillard-Baron, J. *Mol. Phys.* **1974**, *28*, 809.

(48) Yu, J.; Zerner, M. C. *J. Chem. Phys.* **1994**, *100*, 7487.

(49) Ben-Amotz, D.; Herschbach, D. *J. Phys. Chem.* **1993**, *97*, 2295.

(50) Ravi, M.; Samantta, A.; Radhakrishnan, T. P. *J. Phys. Chem.* **1994**, *98*, 9133.

(51) Miertuš, S.; Tomasi, J. *Chem. Phys.* **1982**, *65*, 239.

(52) Linder, B. *J. Chem. Phys.* **1961**, *35*, 371; **1962**, *37*, 963.

(53) (a) Longuet-Higgins, H. C.; Pople, J. A. *J. Chem. Phys.* **1957**, *27*, 192. (b) Kettley, J. C.; Palmer, T. F.; Simons, J. P. *Chem. Phys. Lett.* **1986**, *126*, 107. (c) Shalev, E.; Ben-Horin, N.; Even, U.; Jortner, J. *J. Chem. Phys.* **1991**, *95*, 3147. (d) Shalev, E.; Ben-Horin, N.; Jortner, J. *J. Chem. Phys.* **1992**, *96*, 1848.

(54) Kakitani, T. *Photochem. Photobiol.* **1993**, *58*, 175.

(55) Notice that the ground−excited state transition dipole, usually separated in the Longuett-Higgins/Pople theory, belongs actually to the solute polarizability.

(56) (a) Burrows, B. L.; Amos, A. T. *Theor. Chim. Acta* **1974**, *36*, 1. (b) Das, G. P.; Dudis, D. S. *Chem. Phys. Lett.* **1991**, *185*, 151. (c) Perez, J. J.; Villar, H. O. *Chem. Phys. Lett.* **1992**, *188*, 604. (d) Villesuzanne, A.; Hoarau, J.; Ducasse, L. *J. Chem. Phys.* **1992**, *96*, 495. (e) Kanev, I.; Tasseva, M.; Maruani, J.; Zyss, M. *C. R. Acad. Sci. Paris* **1994**, *318*, 305.

(57) (a) Rérat, M.; Pouchan, C. *Phys. Rev. A* **1994**, *49*, 829. (b) Mérawa, M.; Rérat, M.; Pouchan, C. *Phys. Rev. A* **1994**, *49*, 2493.

(58) (a) *Handbook of Spectroscopy*; Robinson, J. W., Ed.; CRC Press: Cleveland, OH, 1974; Vol. 1. (b) *CRC Handbook of Chemistry and Physics*; Lide, D. R., Ed.; CRC Press: Boca Raton, FL, 1994.

(59) (a) Pierotti, R. A. *J. Phys. Chem.* **1963**, *67*, 1840. (b) Pierotti, R. A. *Chem. Rev.* **1976**, *76*, 717.

(60) Schmid, R.; Matyushov, D. *J. Phys. Chem.* **1995**, *99*, 2393.

(61) (a) Cheng, L.-T.; Tam, W.; Stevenson, S. H.; Meredith, G. R.; Rikken, G.; Marder, S. R. *J. Phys. Chem.* **1991**, *95*, 10631. (b) Cheng, L.-T.; Tam, W.; Marder, S. R.; Stiegman, A. E.; Rikken, G.; Spangler, C. W. *J. Phys. Chem.* **1991**, *95*, 10643.

(62) Richert, R.; Wagener, A. *J. Phys. Chem.* **1993**, *97*, 3146. The treatment contains several approximations: (i) disregard of dispersion forces, (ii) solute polarizability is put to zero, and (iii) the variation in the solvation energy due to the high-frequency modes (the second term in eq 11) has been omitted in the absorption frequency shift.

(63) Miller, K. J. *J. Am. Chem. Soc.* **1990**, *112*, 8533.

(64) (a) Stell, G.; Rasaiah, J. C.; Narang, H. *Mol. Phys.* **1972**, *23*, 393. (b) Stell, G. Equilibrium Techniques. In *Modern Theoretical Chemistry*; Berne, B. J., Ed.; Plenum Press: New York, 1977; Vol. 4, Part A. (c) Wertheim, M. S. *Mol. Phys.* **1979**, *37*, 83. (d) Kriebel, C.; Winkelmann, J. *Mol. Phys.* **1996**, *88*, 559.

(65) Luzhkov, V.; Warshel, A. *J. Am. Chem. Soc.* **1991**, *113*, 4491.

(66) Sinha, H. K.; Yates, K. *J. Am. Chem. Soc.* **1991**, *113*, 6062.

(67) (a) Labhart, H.; Wagnière, G. *Helv. Chim. Acta* **1963**, *46*, 1314. (b) Teng, C. C.; Garito, A. F. *Phys. Rev. Lett.* **1983**, *50*, 350. (c) Hujits, R. A.; Hesselink, C. L. J. *Chem. Phys. Lett.* **1989**, *156*, 209. (d) Matsuzawa, N.; Dixon, D. A. *Int. J. Quantum Chem.* **1992**, *44*, 497.

(68) DeBolt, S. E.; Kollman, P. A. *J. Am. Chem. Soc.* **1990**, *112*, 7515.

(69) The orientational part of the dipole solvation energy is obtained by switching off the solute−solvent and solvent−solvent center-of-mass correlations in the solvent linear response function. The orientational part of solvation is formed by the one-particle dipolar response and the chain solvent−solvent dipole−dipole correlations. The packing component of the solvation energy is the difference between the total solvation energy and the orientational part.

(70) Liao, S. C.; Chan, R. K. *Can. J. Chem.* **1971**, *49*, 2700.

(71) (a) Horng, M. L.; Gardecki, J. A.; Papazyan, A.; Maroncelli, M. *J. Phys. Chem.* **1995**, *99*, 17311. (b) Reynolds, L.; Gardecki, J. A.; Frankland, S. J. V.; Horng, M. L.; Maroncelli, M. *J. Chem. Phys.* **1996**, *100*, 10337.

(72) (a) Andersen, H. C.; Chandler, D.; Weeks, J. D. *Adv. Chem. Phys.* **1976**, *34*, 105. (b) Barker, A.; Henderson, D. *Rev. Mol. Phys.* **1976**, *48*, 587. (c) Pratt, L. R.; Chandler, D. *J. Chem. Phys.* **1977**, *67*, 3683.

(73) Some of the H-bonding effect can be included as higher permanent moments. The quadrupole moment is actually very important for the dielectric properties of water and hydration of small ions; see: Carnie, S. L.; Patey, G. N. *Mol. Phys.* **1982**, *47*, 1129 and ref 16b.

(74) (a) Haberfield, P.; Lux, M. S.; Rosen, D. *J. Am. Chem. Soc.* **1977**, *99*, 6828. (b) Haberfield, P.; Rosen, D.; Jasser, I. *J. Am. Chem. Soc.* **1979**, *101*, 3196.

(75) (a) Brunschwig, B. S.; Ehrenson, S.; Sutin, N. *J. Phys. Chem.* **1986**, *90*, 3657. (b) Hupp, J. T.; Dong, Y.; Blackbourn, R. L.; Lu, H. *J. Phys. Chem.* **1993**, *97*, 3278.

(76) (a) Heitele, H.; Pöllinger, F.; Kremer, K.; Michel-Beyerle, M. E.; Futscher, M.; Voit, G.; Weiser, J.; Staab, H. A. *Chem. Phys. Lett.* **1992**, *188*, 270. (b) Gould, I. R.; Noukakis, D.; Goodman, J. L.; Young, R. H.; Farid, S. *J. Am. Chem. Soc.* **1993**, *115*, 3830.

(77) Oevering, H.; Paddon-Row, M. N.; Heppener, M.; Oliver, A. M.; Cotsaris, E.; Verhoeven, J. W.; Hush, N. S. *J. Am. Chem. Soc.* **1987**, *109*, 3258.

(78) (a) Matyushov, D. V. *Chem. Phys.* **1992**, *164*, 31. (b) Matyushov, D. V. *Chem. Phys. Lett.* **1993**, *203*, 131. (c) Matyushov, D. V.; Ladanyi, B. M. Manuscript in preparation.

(79) Catalán, J.; Mena, E.; Meutermans, W.; Elguero, J. *J. Phys. Chem.* **1992**, *96*, 3615.